Photorespiration and the Evolution of C_4 Photosynthesis

Rowan F. Sage,[1] Tammy L. Sage,[1] and Ferit Kocacinar[2]

[1]Department of Ecology and Evolutionary Biology, University of Toronto, Toronto, Ontario M5S3B2, Canada; email: r.sage@utoronto.ca

[2]Faculty of Forestry, Kahramanmaraş Sütçü İmam University, 46100 Kahramanmaraş, Turkey

Annu. Rev. Plant Biol. 2012. 63:19–47

First published online as a Review in Advance on January 30, 2012

The *Annual Review of Plant Biology* is online at plant.annualreviews.org

This article's doi: 10.1146/annurev-arplant-042811-105511

1543-5008/12/0602-0019$20.00

Keywords

carbon-concentrating mechanisms, climate change, photosynthetic evolution, temperature

Abstract

C_4 photosynthesis is one of the most convergent evolutionary phenomena in the biological world, with at least 66 independent origins. Evidence from these lineages consistently indicates that the C_4 pathway is the end result of a series of evolutionary modifications to recover photorespired CO_2 in environments where RuBisCO oxygenation is high. Phylogenetically informed research indicates that the repositioning of mitochondria in the bundle sheath is one of the earliest steps in C_4 evolution, as it may establish a single-celled mechanism to scavenge photorespired CO_2 produced in the bundle sheath cells. Elaboration of this mechanism leads to the two-celled photorespiratory concentration mechanism known as C_2 photosynthesis (commonly observed in C_3–C_4 intermediate species) and then to C_4 photosynthesis following the upregulation of a C_4 metabolic cycle.

Contents

C_3 photosynthesis: the photosynthetic pathway where CO_2 is directly fixed into three-carbon compounds by RuBisCO

C_4 photosynthesis: a CO_2-concentrating mechanism where PEPC first fixes CO_2 into four-carbon compounds

Ribulose bisphosphate carboxylase/oxygenase (RuBisCO): the primary CO_2-fixing enzyme in plants; it can also oxygenate RuBP, initiating the process of photorespiration

INTRODUCTION

In the past 40 million years, Earth's climate system has changed from a warm, moist world with temperate poles to a cold, somewhat dry planet with polar ice caps, extreme deserts, and widespread grasslands (59, 152). Coupled with this climate shift has been a reduction in the atmospheric CO_2 content from over 1,000 μmol CO_2 mol^{-1} air 50 Mya to less than 200 μmol mol^{-1} 20 kya (7, 133, 152). These changes in the climate and atmosphere caused dramatic evolutionary responses in the planet's biota and contributed to the rise of the modern biosphere (10, 11, 79, 133). Many of these responses occurred in the physiology of plants, reflecting the direct impact of CO_2, temperature, humidity, and water availability on photosynthesis (43, 48, 116).

Among the most profound evolutionary changes was the rise of novel photosynthetic pathways that compensated for deficiencies that appeared in the preexisting C_3 pathway as atmospheric CO_2 declined. These new pathways—C_4 and crassulacean acid metabolism (CAM) photosynthesis—impacted the biosphere by contributing to the rise of new life forms, ecosystems, and vegetation-atmosphere interactions (3, 11, 31, 100, 117). The most prolific of the new modes of photosynthesis was the C_4 photosynthetic pathway, which now accounts for 23% of terrestrial gross primary productivity despite occurring in only 7,500 of the world's 250,000 plant species (120, 129). C_4 photosynthesis represents a complex evolutionary trait that resulted from a major reorganization of leaf anatomy and metabolism to create a CO_2-concentrating mechanism that counteracts the inhibitory effects of low atmospheric CO_2 on photosynthesis (36, 37, 53). The C_4 pathway evolved independently at least 66 times within the past 35 million years, making it one of the best examples of evolutionary convergence in the living world (52, 118). How C_4 photosynthesis evolved and why it did so with such repeatability are two important questions in plant biology. In this review, we examine the latest progress in our understanding of C_4 evolution and discuss this research in the context of earlier hypotheses and speculations (36, 85–87, 108, 117). Of central importance to our current understanding is the role of ribulose bisphosphate carboxylase/oxygenase (RuBisCO) oxygenation and photorespiration, which has been called "the bridge to C_4 photosynthesis" (4).

THE C_4 SYNDROME

C_4 photosynthesis metabolically concentrates CO_2 from the intercellular air spaces of a leaf into an internal compartment where the primary CO_2-fixing enzyme RuBisCO is localized (**Figure 1**). The internal compartment is commonly called the bundle sheath (BS) tissue, because RuBisCO is usually confined to

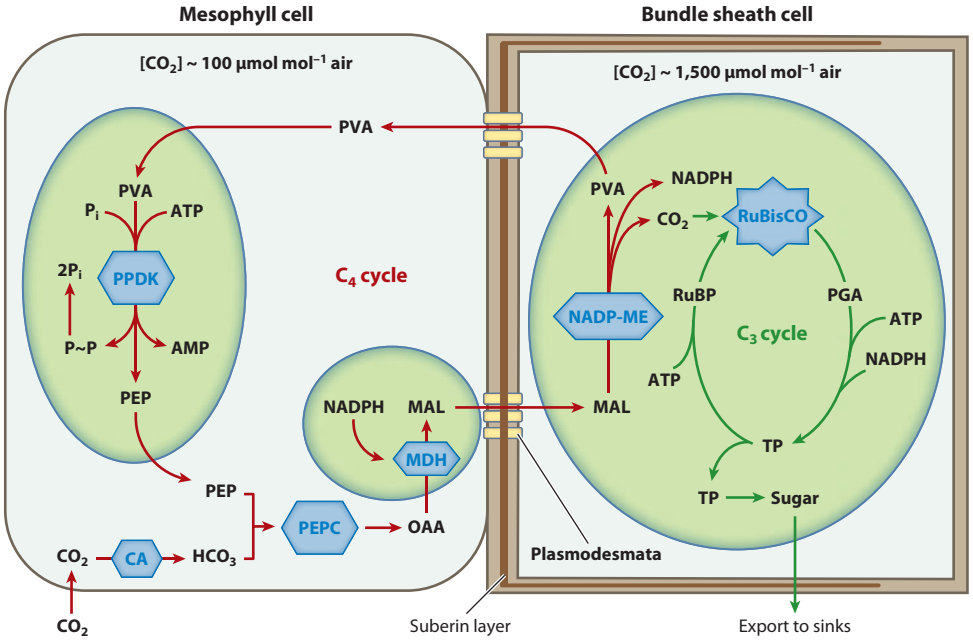

Figure 1

Diagrammatic representation of the C_4 photosynthetic pathway as it occurs in plants of the NADP-malic enzyme (NADP-ME) subtype. All C_4 species initiate the CO_2-concentration process by converting CO_2 to bicarbonate using carbonic anhydrase (CA). The cytosolic enzyme PEP carboxylase (PEPC) fixes the bicarbonate to PEP, forming a four-carbon organic acid, oxaloacetic acid (OAA). PEP carboxylation occurs in the cytosol in an outer cellular compartment, which is chlorenchymatous mesophyll tissue in all but three terrestrial C_4 plant species. OAA is converted to malate (MAL), which diffuses through plasmodesmata into an inner, bundle sheath–like compartment, where it is decarboxylated by NADP-ME, releasing CO_2, NADPH, and pyruvate (PVA). The CO_2 level within the bundle sheath layer can build up to over 10 times the CO_2 level in the intercellular spaces, thereby suppressing the oxygenase activity of RuBisCO that is colocalized in the bundle sheath with the decarboxylating enzyme. RuBisCO refixes the released CO_2 with little interference from the competitive substrate O_2. The PVA diffuses back to the mesophyll cell, where it is phosphorylated to PEP by pyruvate phosphate dikinase (PPDK) using the equivalent of two ATPs. Together, the roughly concentric layers of enlarged bundle sheath–like tissues and mesophyll tissues are termed Kranz anatomy, in reference to their wreath-like arrangement. Green ovals indicate chloroplasts. Additional abbreviations: MDH, malate dehydrogenase; PGA, 3-phosphoglyceric acid; RuBP, ribulose-1,5-bisphosphate; TP, triose phosphate.

a distinct cell layer between the mesophyll (M) cells and the vascular bundles. However, the BS proper is but one of a number of cell layers that have been modified to hold RuBisCO, the decarboxylating enzymes, and the reactions of the C_3 metabolic cycle in the various lineages of C_4 photosynthesis (29). Mestome sheath cells, along with parenchyma cells between M and water-storing tissue, are two examples of non-BS cells that serve as the site of CO_2 concentration in certain C_4 lineages (29, 35).

In addition to variation in the anatomical tissues recruited into the M and BS roles, there is variation in the enzymes recruited into the C_4 metabolic cycle. Three biochemical subtypes of C_4 photosynthesis are recognized based on the principal decarboxylating enzyme used in the BS. These are the NADP-malic enzyme (NADP-ME) subtype, the NAD-malic enzyme (NAD-ME) subtype, and the PEP carboxykinase (PEPCK) subtype (65). Many C_4 species also use a second decarboxylating enzyme,

Bundle sheath (BS): a layer of cells surrounding each vascular bundle; in C_4 plants, RuBisCO is localized to the BS, where CO_2 concentration occurs

Kranz anatomy: a specialized anatomy in which enlarged BS cells and a reduced M tissue form concentric wreaths around the vascular bundles

Mesophyll (M): the major interveinal tissue in leaves; in C_4 plants, initial fixation of CO_2 occurs in the mesophyll

Decarboxylase: an enzyme that releases CO_2 from an organic acid; C_4 plants employ 1 or 2 of 3 decarboxylating enzymes (NADP-ME, NAD-ME, or PEPCK) in BS tissue

Carbon isotope ratios: the ratio of carbon-13 to carbon-12 in a tissue, usually in reference to a standard; C_3 and C_4 species differ in their carbon isotope ratios, allowing for easy identification of the photosynthetic pathway

Phylogeny: a representation of evolutionary relationship based on shared characteristics or gene sequences; phylogenies are commonly represented as tree diagrams

although at reduced activity relative to the principal decarboxylase (45, 65). Associated with the biochemical subtypes are variations in the chloroplast ultrastructure of the BS tissue (53, 65). For example, in BS cells of the NADP-ME subtype, mitochondria numbers are low and chloroplasts are depleted in photosystem II. In BS cells of the NAD-ME subtype, by contrast, mitochondria and photosystem II numbers are high. Some C_4 lineages incorporate a suberin layer into the outer wall of the BS layer, possibly to reduce CO_2 leakage, whereas many do not (29).

Furthermore, C_4 enzymes are often recruited from different ancestral isoforms. In *Flaveria bidentis*, the gene encoding the C_4 carbonic anhydrase (CA) in the cytosol is derived from a chloroplastic ancestor through loss of a transit peptide, whereas in *Cleome gynandra*, a plasma membrane–bound CA is recruited for the C_4 function (77). In the case of PEP carboxylase (PEPC), the C_4 isoform in *Flaveria* derives from the *ppc-2* gene family of PEPC, whereas the C_4 isoforms in *Alternanthera*, *Mollugo*, and *Suaeda* were recruited from the *ppc-1* gene family (25). When all of the variations among the different lineages of C_4 photosynthesis are considered, it is apparent that each evolutionary lineage is unique in some way, and only the initial two steps of C_4 photosynthesis—hydration of CO_2 to bicarbonate and PEP carboxylation—are common to all lineages (68). The C_4 pathway is thus more appropriately considered a syndrome, because it does not result from one specific biochemical pathway or anatomical structure but rather represents "a combination of traits that produce a characteristic outcome" (from the second abbreviation for syndrome in the *Oxford English Dictionary*). For all but two lineages of C_4 plants, the characteristic combination of traits results in the energy-dependent concentration of CO_2 around RuBisCO within an inner tissue compartment. In the two exceptions, C_4 photosynthesis occurs within a single cell, with the inner compartment where CO_2 is concentrated being either in the middle of the cell (*Bienertia* lineage) or along the inner pole of an elongated cell (*Suaeda aralocaspica* lineage) (35).

FREQUENCY OF C_4 ORIGINS

Although it has long been recognized that the C_4 syndrome evolved on multiple occasions (96, 128), the high repeatability of C_4 evolution was not fully realized until the past decade, when molecular phylogenies and detailed surveys of carbon isotope ratios clarified C_3 and C_4 relationships in the clades where the C_4 pathway occurs (**Figure 2**). An early treatment proposed that C_4 photosynthesis independently evolved approximately 20 times (128). More recently, in the first comprehensive analysis using molecular phylogenies, Kellogg (68) estimated that there are 31 distinct lineages of C_4 photosynthesis. Kellogg's analysis was hampered by incomplete species representation within phylogenies, limited knowledge of photosynthetic pathway in many families, and difficulty distinguishing independent origins from reversion; since then, and in part because of Kellogg's study, detailed phylogenetic and carbon isotope studies have resolved C_3, C_4, and C_3–C_4 intermediate relationships within many taxonomic groups (8, 23, 24, 40, 78, 112, 118, 122, 124, 146, 147). Genomic analysis of protein evolution has also been exploited to differentiate C_4 origins where molecular phylogenies provide insufficient resolution (22, 25). Such approaches have been able to estimate 22–24 distinct C_4 lineages in the grass family (Poaceae), which contains 4,500 C_4 species (11, 22, 23, 52, 138); 6 distinct lineages in the sedges (Cyperaceae), the second-largest family of C_4 plants, with an estimated 1,500 species (8, 112); and up to 10 lineages in Chenopodiaceae, the most speciose C_4 family of eudicots, with about 500 C_4 species (64, 118, 120). There are approximately 1,500 C_4 species in the eudicots (120). Phylogenetic studies have also identified multiple C_4 origins within genera. The sedge genus *Eleocharis* has two independent lines (8, 112). In the eudicots, three distinct C_4 lineages are present within *Cleome* (Cleomeaceae), including that of the new model C_4 plant

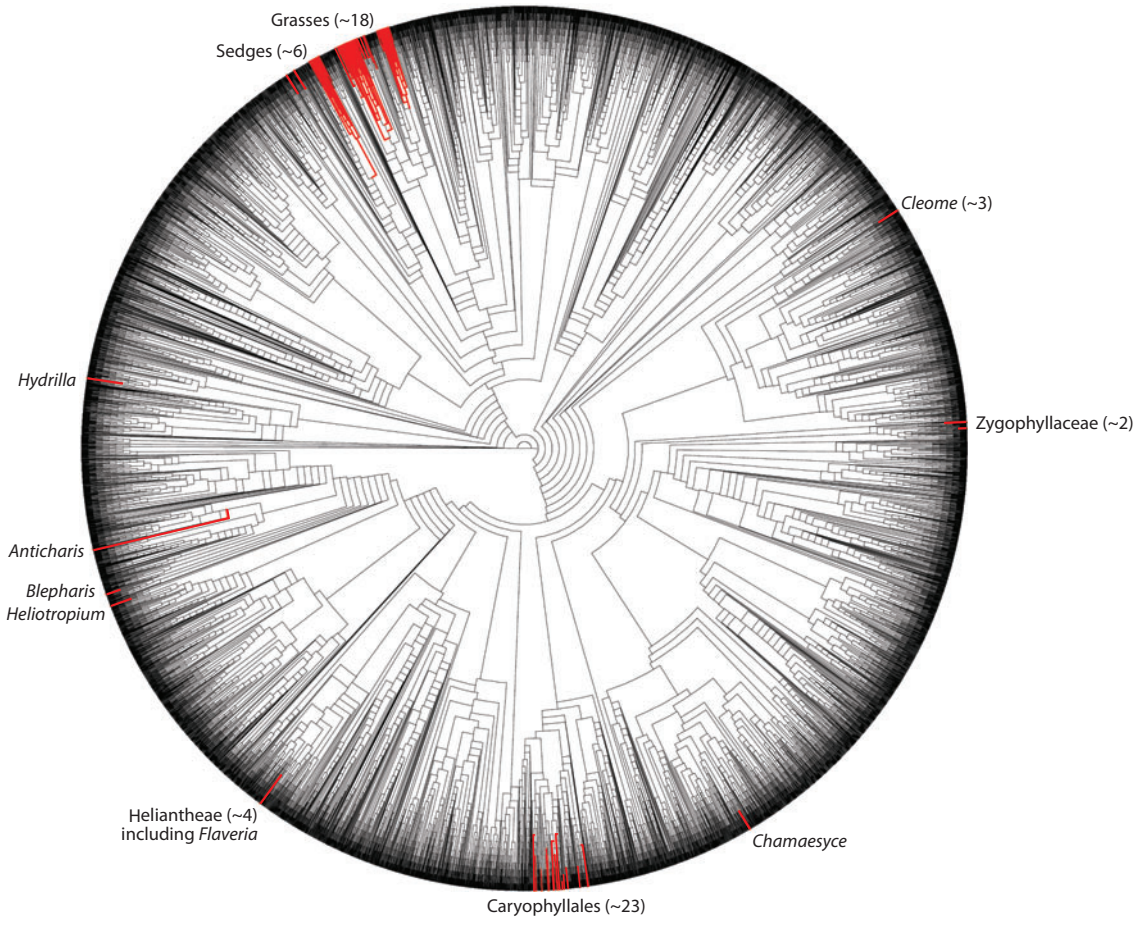

Figure 2

The phylogenetic distribution of 47 angiosperm clades with C_4 photosynthesis. Red branches indicate C_4 lineages, and dark-gray branches indicate C_3 lineages. The numbers besides the taxonomic names indicate the number of independent origins in that clade. Taken from Reference 118 with permission.

C. gynandra (40). One line originated in Australia, a second in northeast Africa/Arabia, and a third in South Africa; surprisingly, all three have just one species each (40). In *Suaeda* (Chenopodiaceae) there are four distinct C_4 origins, including two where the C_4 pathway operates within single cells (70). *Mollugo* (Molluginaceae) presents an interesting case of two postulated origins of C_4 photosynthesis in a single taxonomic species, *Mollugo cerviana* (25).

In total, 62 distinct lineages of C_4 photosynthesis are listed in a recent survey (118). All of the C_4 lines occur in the angiosperms, with a total of 26 monocot and 36 eudicot lineages. These numbers are up from 48 independent origins estimated by Sage (117) and will likely increase in the near future. Four to six additional lineages have already been identified in the grasses since Sage et al.'s (118) study published in 2011, bringing the current number of known lineages to 66–68 (52). Within the angiosperm phylogenetic tree, many of the C_4 lineages are clumped together, with grasses and sedges accounting for all but 1 of the monocot lines and the eudicot order Caryophalales accounting for 23 of the 36 C_4 eudicot lines (**Figure 2**). In the grasses, all C_4 lineages occur within the branch of the family termed

Miocene: a geological epoch occurring 5–23 Mya

Oligocene: a geological epoch occurring 23–34 Mya

the PACMAD [named for the subfamilies Panicoideae, Arundinoideae, Chloridoideae, Micrairoideae, Aristidoideae, and Danthoideae (68)]. At the family level, there are 19 families containing C_4 plants, and of these, 4 (Poaceae, Cyperaceae, Chenopodiaceae, and Amaranthaceae) account for two-thirds of the lineages (118). These patterns indicate the presence of factors that predispose certain groups to repeatedly evolve C_4 photosynthesis. The nature of the facilitating factors is unknown but probably relates to ecological drivers, genetic attributes, and structural features of the ancestral C_3 leaf (85, 117).

WHEN DID C_4 PHOTOSYNTHESIS APPEAR?

It has long been hypothesized that C_4 photosynthesis evolved in terrestrial plants relatively recently in geological time (37, 96, 119, 128). Recent work confirms this possibility. Numerous fossil and isotopic studies demonstrate a widespread expansion of C_4-dominated ecosystems beginning approximately 10 Mya (18, 19, 131, 133). By 5–7 Mya, mixed C_3 and C_4 savannas had become common across Africa, Asia, and the Americas, culminating in C_4-dominated grasslands at low latitude approximately 2–3 Mya (18, 80, 127, 131). Expansion of the C_4 grasslands in the late Miocene (10–6 Mya) is proposed to result from increased aridity, seasonality, fire frequency, and an additional reduction in atmospheric CO_2 from above 400 μmol mol^{-1} to below 300 μmol mol^{-1} (3, 6, 31, 67, 131). The oldest macrofossils of identifiable C_4 plant parts date back to 12–15 Mya (18), whereas soil carbonates shift toward a C_4 carbon isotope ratio beginning approximately 23 Mya in North America (41, 42). Well-preserved silica bodies (phytoliths) indicate that C_4 grasses were present on the North American landscape by 19 Mya (130), whereas carbon isotope ratios of fossilized pollen suggest the presence of C_4 grasses in southwest Europe by 33 Mya (137). A few studies propose much earlier origins of C_4 photosynthesis on the basis of isotopic excursions in fossil carbon (75, 151); however, these studies lack complementary evidence and thus remain suggestive (18, 117).

A limitation of the geological evidence is that the fossil and isotopic records are unlikely to include uncommon species, such as newly evolved C_4 plants. To estimate the earliest origins, the best technique currently available is a molecular clock analysis of the DNA sequences from phylogenetic studies. Using molecular clock approaches, the earliest C_4 origin is estimated to have occurred in the grass subfamily Chloridoideae during the mid-Oligocene epoch, approximately 30 Mya (**Figure 3**) (11, 23, 138). The oldest C_4 dicot lineage is Caroxyloneae in the Chenopodiaceae family, with stem and crown node ages of 22–25 Mya (24). The oldest C_4 sedge lineage, *Bulbostylis*, dates from 10–20 Mya (8). Additional C_4 origins occur over the following 20–30 million years (**Figure 3**). Higher probabilities of origin occur during the Oligocene–early Miocene transition (25 Mya), the mid-Miocene epoch (15 Mya, during a climatic warm spell), and approximately 5 Mya (21, 25, 138). The

Figure 3

(*a*) The estimated ages of 56 monocot and dicot lineages of C_4 plants, modeled after References 23, 24, 26, and 101. The left end of each bar represents the age of the stem node for each lineage, the right end of each bar is the crown node, and the circle represents the median age. (*b*) Atmospheric CO_2 concentrations and mean oxygen isotope ratios ($\delta^{18}O$) over the past 46 million years. CO_2 concentrations are from marine and lacustrine proxy estimates; oxygen isotopes are based on marine foraminifera extracted from deep sea cores (from the median values in Reference 152, figure 2). This panel also shows the appearance time of fossilized material with C_4 carbon isotope signatures and C_4-dominated ecosystems (31, 131). On average, low $\delta^{18}O$ values indicate warm, moist climates over the planet, whereas high values correspond to cold, dry climates. These records show that the planet dramatically cooled from the Eocene to the Pleistocene. Abbreviations: Plio, Pliocene; Pl, Pleistocene.

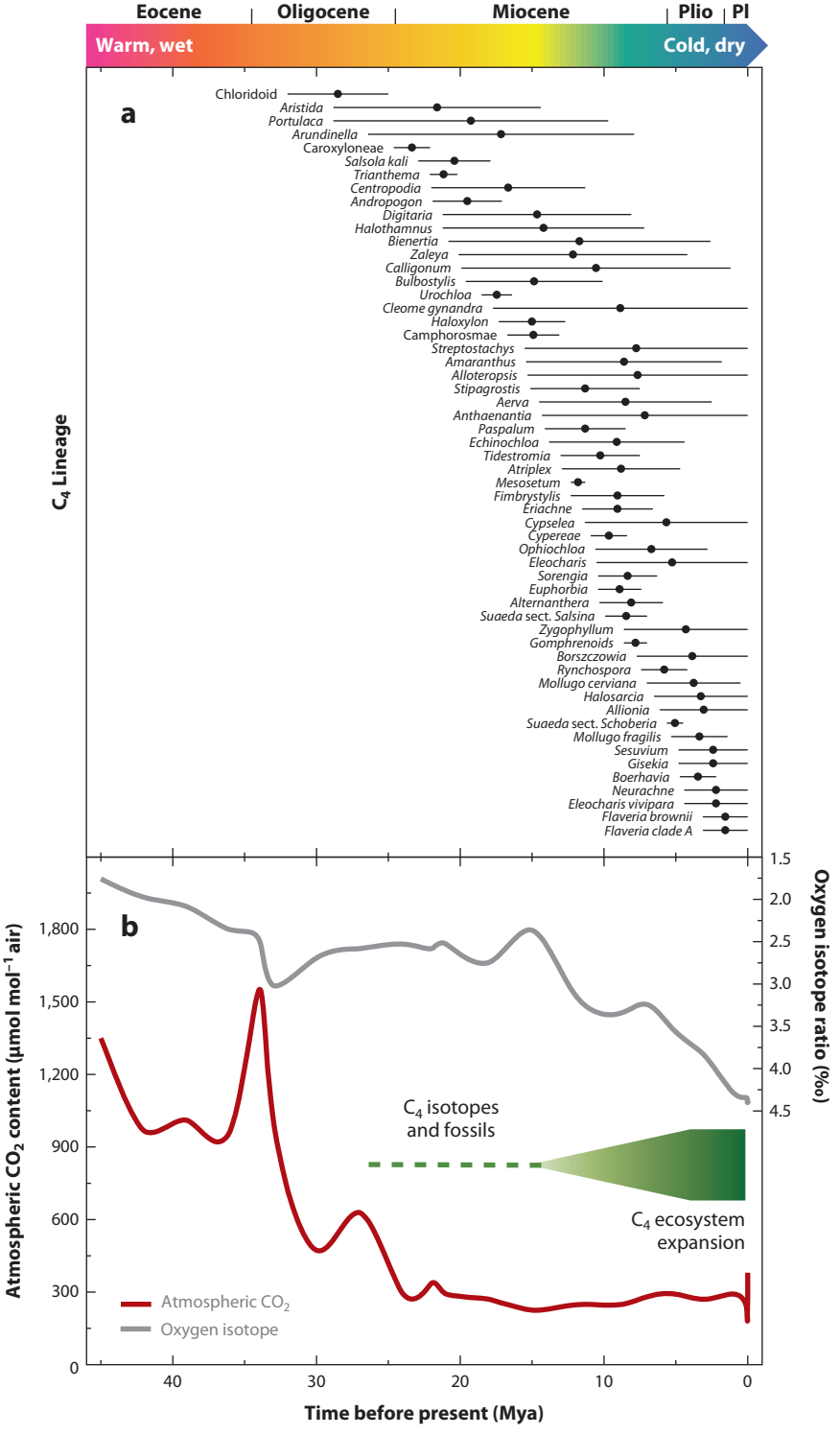

youngest C_4 lineages are *Neurachne* in the grasses and *Flaveria* in the eudicots, both of which are estimated to have evolved in the past 5 Mya (**Figure 3**) (24). Both genera have extant species that qualify as evolutionary intermediates between the C_3 and C_4 condition, with *Flaveria* having nine C_3–C_4 intermediate species (118). Because of its large number of C_3–C_4 intermediates, *Flaveria* has become the leading model for studies of C_4 evolution.

Comparisons between the time of C_4 emergence and that of major geological events demonstrate a strong correlation between the probability of a C_4 origin and low atmospheric CO_2 content (23, 24). Atmospheric CO_2 concentration is estimated by models and various proxies to have exceeded 1,000 μmol mol^{-1} between 35 and 55 Mya, after which it declined to near current levels (390 μmol mol^{-1}) by approximately 25 Mya (**Figure 3**) (133, 152). A second reduction in CO_2, to near 300 μmol mol^{-1}, is proposed to have occurred between 10 and 15 Mya (74, 134), which precedes the expansion of the C_4 grasslands at low latitudes, a late-Miocene/Pliocene burst of C_4 evolution, and a burst of radiation in CAM groups (3). In parallel with the CO_2 decline, climate conditions changed from the warm, wet world of the Eocene (55–34 Mya) to the cool, relatively dry world of the early Miocene (23–20 Mya) (**Figure 3**) (152). The climate further deteriorated in the late Miocene and into the Pleistocene (10–2 Mya), culminating in a world that on average was cold and dry but still warm at low latitudes (152).

Decreasing atmospheric CO_2 has been hypothesized to be the primary trigger for the evolution of C_4 photosynthesis, through what is known as the carbon starvation hypothesis (36, 37, 85, 117). The initial version of this hypothesis proposed that C_4 species originated in the late Miocene, when carbon isotope evidence demonstrated that C_4 plants expanded across low latitudes (19, 36, 37). This isotopic shift is now recognized as reflecting the expansion of preexisting C_4 graminoid species rather than their origin (6, 31, 67, 117). In the 1990s, improved estimates of atmospheric CO_2 change showed that the CO_2 decline from high Cretaceous values to low values of recent geological time mainly occurred in the Oligocene (34–23 Mya) rather than the late Miocene (133, 153). This led to proposals that C_4 plants first evolved in the late Oligocene (6, 116, 117, 133), a possibility initially supported by early molecular clock studies indicating that C_4 photosynthesis was present in the grass subfamily Andropogoneae by 25 Mya (46, 68). With the molecular clock evidence now indicating that all of the C_4 lineages evolved after the Oligocene CO_2 decline, the carbon starvation hypothesis has received critical support (8, 11, 23–25, 138).

ENVIRONMENTAL CORRELATES OF C_4 EVOLUTION

In its original version, the carbon starvation hypothesis proposed that low CO_2 was a trigger for C_4 evolution by causing high rates of photorespiration in warm climates, thereby reducing photosynthetic efficiency of the C_3 flora (36, 37). The 30-million-year spread in the timing of the many C_4 origins following the Oligocene CO_2 decline now indicates that rather than serving as a trigger, low CO_2 was a precondition for C_4 evolution, enabling other factors to play a pivotal role. Factors proposed to operate in concert with, or instead of, low CO_2 in promoting C_4 evolution include heat, aridity, high light, salinity, and ecological disturbance (32, 96, 100, 116, 117). Phylogenetically informed comparisons between the habitats of C_3 and C_4 PACMAD grasses implicate high light and warm temperatures as the leading environmental factors contributing to C_4 evolution (32, 100). Aridity does not correlate with species habitat in the phylogenetic analyses, leading to suggestions that it had an indirect effect by opening canopies and promoting fire (32).

Another approach to addressing the environmental conditions promoting C_4 evolution is to examine the field habitats and microclimates of extant species that branch at the phylogenetic nodes across which the transition from C_3 to C_4 photosynthesis occurs. The habitats of C_3 and C_3–C_4 intermediate species that branch

at these nodes should reflect the environmental factors promoting C_4 evolution. Using this approach, researchers determined that C_4 photosynthesis in 32 lineages most likely arose in monsoon-affected regions of warm-temperate to tropical latitudes (118, 124). These areas are currently hot during the summer yet receive periodic monsoon rainfall to support a summer growing season. For most of these areas, the summer heat and drought of modern times extend back to at least the Miocene (131, 149). In particular, all of the C_3–C_4 intermediate species are summer-active and occur in areas with high evaporative demand (**Table 1**). Although most also occur in regions with frequent drought or elevated salinity, some are found on moist soils—for example, *Flaveria chlorofolia* and *Heliotropium lagoense*. Competition tends to be low owing to recent disturbance, severe abiotic stress, or extreme soil type (**Table 1**). As an example, *Flaveria floridana* (C_3–C_4) occurs in disturbed or saline flats along the Gulf Coast of the Americas, persisting for only a few years until excluded by perennial vegetation (87). It regularly photosynthesizes above 35°C (87). Its closest C_3 relatives occur in subtropical Mexico along the Pacific coast (*Flaveria robusta*) or central Mexico (*Flaveria pringlei*), typically growing in disturbed areas of semiarid scrub vegetation (104, 132).

C_3–C_4 intermediate: technically, a plant that is phylogenetically intermediate between C_3 and C_4 species; however, the term commonly refers to any plant with C_2 photosynthesis

The consistent feature of the hot, monsoon-affected environments occupied by the

Table 1 The evolutionary lineages of C_3–C_4 intermediate photosynthesis and their current habitats[a]

Lineage	Number of species	Habitat	Reference
C_3–C_4 intermediate photosynthesis precedes C_4 photosynthesis in a phylogeny			
Bassia sedoides (Chenopodiaceae)	1	Saline or alkaline meadows; Central Asia	64
Alternanthera (Amaranthaceae)	2	Disturbed, semiarid to moist soils; subtropics	33
Cleome paradoxa (Capparidaceae)	1	Arid, rocky soils; northeast Africa and Arabian Peninsula	40
Euphorbia acuta (Euphorbiaceae)	2	Disturbed, semiarid limestone soils; Texas	124
Flaveria clade A (Asteraceae)	1	Disturbed, semiarid scrub or weed lots; Mexico	104
Flaveria clade B	7	Disturbed, semiarid scrub, saline marshes; Mexico, Texas	104
Flaveria sonorensis	1	Disturbed, semiarid soils; northwest Mexico	104
Heliotropium I (Boraginaceae)	2	Semiarid to arid sandy soils; Mexico, southwest United States	44
Heliotropium II	2	Semiarid sand, gravel or clay flats, mudflats; Americas	44
Mollugo nudicaulis (Molluginaceae)	2	Disturbed, barren soils; widely distributed at low latitudes	25
Nuerachne minor (Poaceae)	1	Arid soils, often shallow; central subtropical Australia	105
C_3–C_4 intermediate photosynthesis is present, but the phylogenetic relationships are unclear			
Portulaca cryptopetala (Portulacaeae)	1	Weedy, disturbed soils of subtropical Argentina, Paraguay, and Bolivia	83
C_3–C_4 intermediate photosynthesis is present in these groups that are not directly ancestral to C_4 species			
Diplotaxis (Brassicaceae)	1	Disturbed, waste soils, sandy soils; southern Europe	83
Mollugo verticilata (Molluginaceae)	1	Hot, disturbed, and barren soils; warm-temperate to tropical regions	25
Moricandia (Brassicaceae)	5	Arid regions; Israel, Egypt	33
Parthenium (Asteraceae)	1	Disturbed, mainly dry or saline soils, widespread weed	56
Salsola (Chenopodiaceae)	1	Arid slopes; Central Asia	47
Steinchisma (Poaceae)	6	Moist soils; warm-temperate to tropical regions	154

Names in boldface are known to have bundle sheath–specific glycine decarboxylase. Table developed from Reference 118 and the reference listed in each row.
[a]C_3–C_4 intermediate photosynthesis is more precisely known as C_2 photosynthesis, as explained in the RuBisCO Oxygenation and Photorespiration section, below.

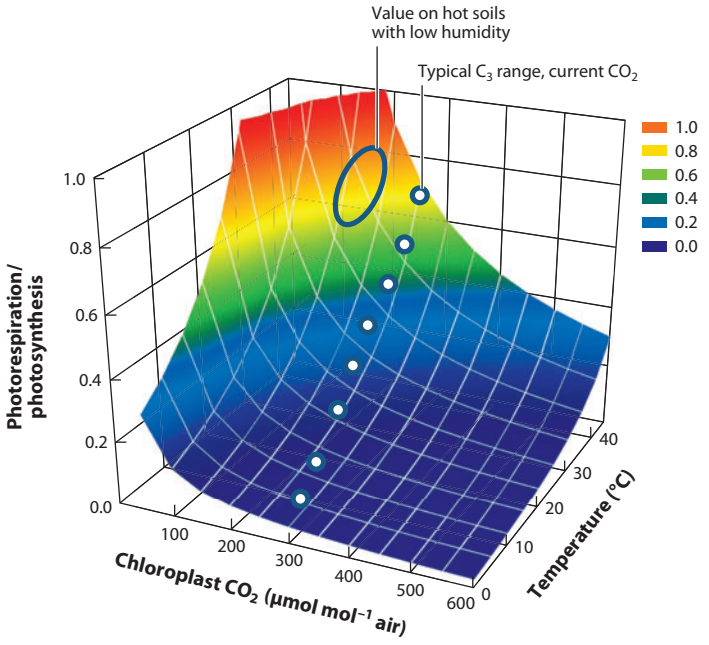

Figure 4

The theoretical response of photorespiration/photosynthesis in C_3 plants as a function of chloroplast concentrations of CO_2 and temperature. Circles show typical values corresponding to nonstressed leaves at current atmospheric CO_2 levels; the oval indicates the values expected for plants in hot environments with low humidity. Figure modeled according to References 37 and 63 using the equation photorespiration/photosynthesis $= O/(S_{rel}C)$, where O and C are the O_2 and CO_2 concentrations in the chloroplast stroma, respectively, and S_{rel} is the specificity of RuBisCO for CO_2 relative to O_2.

transitional species is that photorespiration would be high in C_3 plants owing to elevated leaf temperatures and depressed intercellular CO_2 values. Photorespiration relative to photosynthesis equals $0.5O/(S_{rel}C)$, where O and C are the O_2 and CO_2 concentrations in the chloroplast stroma, respectively, and S_{rel} is the specificity of RuBisCO for CO_2 relative to O_2 (63). Rising leaf temperature reduces S_{rel} while increasing O/C (63). Leaf temperature is enhanced by high air temperature; large radiation loads from direct and reflected sunlight; high infrared emission from hot, barren soil; and reduced stomatal conductance, which reduces evaporative cooling. Low intercellular CO_2 levels result from low atmospheric CO_2 and reduced stomatal conductance caused by drought, salinity stress, and low humidity (125). Warm, dry climates with reduced atmospheric humidity promote large leaf-to-air vapor-concentration differences (VPDs), often above 4 kPa. Reductions in stomatal conductance with VPD increases of 3–5 kPa are typically large, exceeding 50% (125). In *F. floridana* and *Yucca glauca*, for example, VPD values over 3 kPa reduce stomatal conductance by 40%–75%, which in turn causes the intercellular CO_2 level to decline from approximately 240 μmol mol^{-1} to near 160 μmol mol^{-1} (87, 113).

Models of photorespiration illustrate the impact of CO_2 variation, elevated temperature, and low humidity on the photorespiratory potential of C_3 vegetation (**Figure 4**). At elevated CO_2 (>1,000 ppm), photorespiration is minor at all temperatures. At chloroplast CO_2 levels corresponding to current atmospheres, photorespiration exceeds 25% of the photosynthesis rate above 30°C–35°C, assuming stomatal conductance is regulated to give C_i/C_a (intercellular CO_2 partial pressure to ambient CO_2 partial pressure) values of 0.7–0.8, which are typical in nonstressed C_3 vegetation (117). With the expected level of stomatal closure that would occur in hot, semiarid climates, photorespiration/photosynthesis would be well above 40% at 35°C–40°C, particularly in low-CO_2 atmospheres of recent geological time, when CO_2 concentrations were below 300 μmol mol^{-1} (133, 152). Expressed another way, photorespiration rates exceeding 10–15 μmol m^{-2} s^{-1} could be expected in plants such as *F. pringlei*, which have carboxylation capacities of 20–30 μmol m^{-2} s^{-1} above 30°C. This magnitude of photorespiration produces an abundance of CO_2 that could be an important resource if a plant were able to trap and refix it before it diffuses out of the cell.

In combination, the habitats of origin for the C_4 lineages of the world support the hypothesis that high photorespiration was the primary driver of C_4 evolution. By promoting photorespiration, low CO_2, elevated temperature, high light, low humidity, drought, and salinity are all contributing factors, particularly in combination. High rates of photorespiration would depress the productivity and fitness of C_3 vegetation, and in the extreme could lead to poor

survival (17, 27, 48). Depression of C_3 productivity, however, is not by itself a satisfactory explanation for how the C_4 pathway evolved. To be robust, a photorespiratory explanation must demonstrate how high rates of photorespiration promoted the evolutionary assembly of the C_4 pathway.

RUBISCO OXYGENATION AND PHOTORESPIRATION

RuBisCO is a dual-function enzyme that oxygenates and carboxylates ribulose-1,5-bisphosphate (RuBP). Oxygenation of RuBP produces 3-phosphoglyceric acid (PGA) and phosphoglycolate (PG). PGA can immediately be recycled back to RuBP via the Calvin cycle, whereas PG is metabolized first to pyruvate and then to PGA via the reactions of the photosynthetic carbon oxidative cycle, which is commonly referred to as photorespiration (4). In photorespiratory metabolism, one-fourth of the carbon in the PG pool is lost as CO_2 in the conversion of two glycine molecules to one serine by the glycine decarboxylase (GDC)–serine hydroxymethyltransferase (SHMT) complex in the mitochondria. In conditions promoting high rates of photorespiration, the flux of CO_2 out of the mitochondria would be substantial, and thus would be an important source of CO_2 if plants could channel it back into the chloroplasts for refixation.

Trapping and refixing photorespired CO_2 becomes possible if plants are able to localize GDC into an interior compartment from which CO_2 efflux could be slowed by large vacuoles, chloroplasts, and thick cell walls. In the M cells of C_3 plants, this can be accomplished by locating mitochondria toward the interior of the cell, inside of a peripheral layer of chloroplasts. For example, in rice, a C_3 grass of warm climates, chloroplasts and chloroplast extensions form a barrier around the periphery of the M cells, whereas the mitochondria are located in the interior of the cell and are often surrounded by chloroplasts (123). This arrangement apparently forces photorespired CO_2 to diffuse out through the chloroplast stroma, where it could be reassimilated. Such a mechanism explains in part the refixation rates of up to 50%–80% of photorespired CO_2 observed in C_3 plants (5, 55, 76, 102).

Another way to recapture photorespired CO_2 is to restrict GDC activity to an internal tissue where thick walls and large vacuoles could slow CO_2 efflux, thereby causing the photorespired CO_2 to accumulate and allowing any nearby RuBisCO to operate with high efficiency. In high-photorespiratory conditions, the production of photorespired CO_2 in an internal compartment would theoretically be large enough to boost CO_2 levels by two- to threefold (14, 142, 144). Spatial separation of RuBisCO oxygenation and glycine decarboxylation is now recognized as the basis for a distinct CO_2-concentrating mechanism in land plants, which has been variously termed glycine shuttling, photorespiratory CO_2 concentration, C_3–C_4 intermediacy, and (recently) C_2 photosynthesis (**Figure 5**). C_3–C_4 intermediacy is the most commonly used name, but is problematic because numerous species using this CO_2-concentrating mechanism are not related to C_4 species, and hence are not true evolutionary intermediates (**Table 1**). In addition, evolutionary intermediacy between C_3 and C_4 species may involve more than glycine shuttling. Because of these concerns, Vogan et al. (139) proposed calling photorespiratory CO_2 concentration "C_2 photosynthesis" to emphasize its status as a distinct CO_2-concentrating mechanism. The term C_2 photosynthesis has the advantage of not automatically being associated with C_4 evolution yet being logically consistent with use of the term C_4 photosynthesis. Both C_2 photosynthesis and C_4 photosynthesis refer to the number of carbons in the metabolite that shuttles CO_2 into an internal compartment. C_2 photosynthesis also follows from the abbreviated name for photorespiration, the C_2 cycle (4).

C_2 PHOTOSYNTHESIS IN HIGHER PLANTS

Approximately 40 species in 21 lineages of vascular plants are currently known to utilize the C_2 photosynthetic pathway (118). Of these, 12

Glycine decarboxylase (GDC): the enzyme complex in photorespiratory metabolism that converts glycine to serine, ammonia, and CO_2

C_2 photosynthesis: a CO_2-concentrating mechanism in which photorespiratory glycine is shuttled into the BS cells for decarboxylation; the released CO_2 enhances carboxylation and suppresses oxygenation by BS RuBisCO

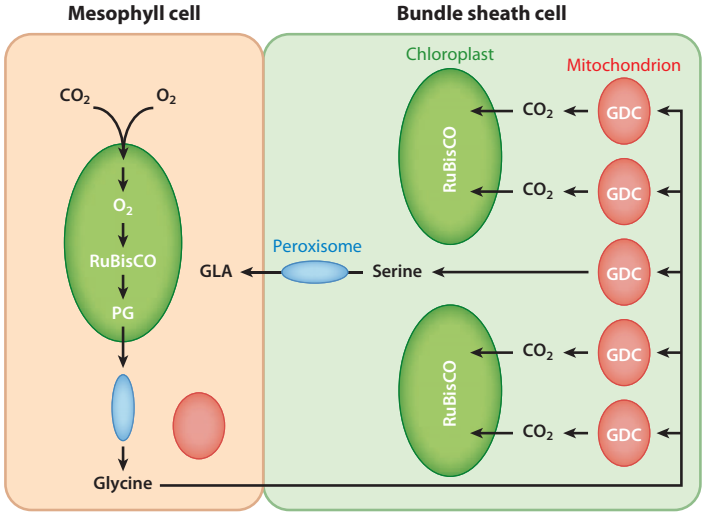

Figure 5

Schematic of C_2 photosynthesis. Phosphoglycolate (PG) produced by the RuBisCO oxygenase reaction is converted to glycine in the peroxisomes of either the mesophyll or bundle sheath cells. The glycine then diffuses to the centripetal mitochondria of the bundle sheath cells to be metabolized to serine and CO_2 by glycine decarboxylase (GDC). The CO_2 released is refixed by bundle sheath chloroplasts, while the serine is converted back to glyceric acid (GLA) in either bundle sheath or mesophyll peroxisomes. The GLA is then converted to ribulose-1,5-bisphosphate (RuBP) in the mesophyll chloroplast. Adapted from Reference 111 with permission.

occur in phylogenetic branches that are sister to C_4 lineages, indicating potential ancestry; however, 9 are separate enough within a phylogeny to indicate no ancestry to C_4 species (**Table 1**) (25, 118). Most of the known C_2 lines occur in the eudicots; only 4 occur in the monocots. The number of documented lineages is probably well below the actual total, because identification of a C_2 plant requires time-consuming anatomical, biochemical, or gas exchange measurements of living plants. C_2 and C_3 plants have similar carbon isotope discrimination values, so rapid carbon isotope screens of herbarium specimens cannot be used to identify C_2 species as they can with C_4 species (92, 122, 143). Although some C_2 species evolved long ago and are ecologically successful [the widespread weed *Mollugo verticillata* is up to 20 million years old (24)], the C_2 pathway is the least common carbon-concentrating mechanism in the plant kingdom. *M. verticillata*, for example, is the only known C_2 species in its clade (24). The most speciose clade of C_2 species, *Flaveria*, has nine C_2 species, whereas the next-most-speciose clades have five or fewer C_2 species (81, 99). This contrasts with the dozens to hundreds of species present in many of the CAM and C_4 lineages (120, 150).

In all lineages of C_2 plants that have been examined, BS or mestome sheath tissue is the site of glycine decarboxylation and CO_2 concentration (90, 124), although the ancestors of single-celled C_4 species may have operated a C_2 pathway between the periphery and innermost region of individual cells (35). Immunolocalizations of antibodies raised against the four subunits of GDC show little P-subunit expression in M cells of C_2 species of *Flaveria*, *Mollugo*, *Moricandia*, and *Steinchisma* (formerly *Panicum*) (61); *Cleome* (78, 146); *Diplotaxis* (135); *Euphorbia* (124); *Heliotropium* (99); *Portulaca* (147); and *Salsola* (145). In C_2 species of *Flaveria* and *Steinchisma*, the H, L, and T subunits of GDC are also absent from the M (97). In C_3–C_4 *Alternanthera tenella* leaves, BS cells have nine times the activity of GDC as M cells (30). The molecular mechanism for the loss of M GDC expression has been examined only in C_3 and C_4 *Flaveria* species. In C_4 *Flaveria trinervia*, the strength and location of GDC expression are controlled by a 1,571-base-pair region in the promoter of the P subunit of the GDC protein (39). The enhancer sequence is located within promoter region 1 between base pairs −1,571 and −1,339, whereas region 3 between base pairs −1,138 and −927 and part of region 6 contain *cis*-regulatory elements that repress M expression of *gdcpA* (39). The nature of the base-pair changes in regions 3 and 6 is unknown, but could involve just a few nucleotide substitutions (39).

Associated with the loss of M expression of GDC in C_2 plants is a pronounced alteration of leaf anatomy and BS ultrastructure that is interpreted to facilitate rapid flux of photorespiratory metabolites between the M and BS compartments as well as the trapping of photorespired CO_2 in a centripetal location of the BS cell (90). With one exception, all C_2 species examined have a pronounced enhancement of

mitochondrial number and/or area in the BS cells, and they are localized to the centripetal (inner) wall region of the BS cell (13, 15, 58, 78, 90, 94, 99, 124, 145–147). The exception occurs in the grass *Neurachne minor*, which has mestome sheath cells filled with organelles but does not position the mitochondria against the inner wall (54). A suberin layer in the wall of the mestome sheath in *N. minor* may trap photorespired CO_2 in the sheath, reducing the need to localize mitochondria in a centripetal position (54). Chloroplast numbers are also increased, and although chloroplasts may be arrayed around the entire cell periphery, there is always a close association between numerous chloroplasts and a rank of mitochondria along the inner wall (13, 15, 58, 78, 90, 94, 99, 108, 124, 135, 145–147). The number of M cells per BS cell is reduced below typical C_3 values (81, 99, 124), and the BS cells are often, but not always, increased in size compared with C_3 relatives (81, 94, 99, 124, 135). Together, glycine shuttling and structural changes boost refixation of photorespired CO_2 to 75%–90% and allow the leaves to lower the CO_2 compensation point of photosynthesis (Γ) to values that are 20%–50% of C_3 values at a given temperature (5, 16, 28, 33, 54, 72, 94, 107, 124, 135, 139, 141, 145–147). The reduction in the CO_2 compensation point increases net CO_2 assimilation rate at low CO_2 levels relative to C_3 species, but generally does not increase CO_2 uptake at elevated CO_2. In C_3–C_4 intermediates of *Alternanthera*, *Euphorbia*, *Flaveria*, *Neurachne*, and *Portulaca*, advantages in net CO_2 assimilation observed at low atmospheric CO_2 are absent above the current atmospheric CO_2 concentration (54, 88, 124, 139, 140, 141, 147). With the continuing increase in anthropogenic CO_2 emissions, the present time in history appears to represent a transition to conditions where the advantage of C_2 photosynthesis is lost.

MODELS OF C_4 EVOLUTION

Photorespiratory CO_2 concentration into the BS was first proposed in 1984 to explain the function and evolutionary significance of the BS structure observed in C_3–C_4 intermediate species (86). In the subsequent decade, Rawsthorne and colleagues (61, 97, 108, 110, 111) confirmed GDC localization to centripetally placed BS mitochondria in *Flaveria*, *Mollugo*, *Moricandia*, and *Panicum* species and provided experimental support for the C_2 pathway as it is currently understood. Subsequently, conceptual models based on their results proposed that the evolution of C_4 photosynthesis first involved the establishment of the C_2 pathway, after which the C_4 metabolic cycle replaced the C_3 cycle operating in the M tissue (84, 87, 90, 108, 117). Although specific steps in these models were based on characteristics of C_2 species from *Flaveria*, *Moricandia*, *Neurachne*, and *Panicum*, there was little phylogenetic information to evaluate the models. The possibility that the putative C_3–C_4 intermediate species represented evolutionary dead ends could not be ruled out.

The past publication of numerous detailed phylogenies now makes it possible to update the evolutionary models of C_4 photosynthesis to account for phylogenetic relationships. Furthermore, the identification of new C_2 species, and C_3 species that are sister to C_2 and C_4 species, has provided additional opportunities to evaluate pathways of C_4 evolution (99, 118, 124, 146, 147). On the basis of this information, we present a conceptual model of C_4 evolution that updates earlier models (90, 117). Our model proposes the following five distinct phases of C_4 evolution (**Figures 6** and **7**): (*a*) preconditioning; (*b*) the evolution of proto-Kranz anatomy; (*c*) the evolution of C_2 photosynthesis; (*d*) the establishment of the C_4 metabolic cycle with the corresponding localization of the C_3 cycle to the BS, marking the beginning of C_4 photosynthesis; and (*e*) an optimization phase, in which Kranz anatomy and leaf biochemistry are modified to maximize the efficiency of the C_4 pathway.

Proto-Kranz anatomy: a condition in C_3 plants in which vein density is enhanced and BS cells are enlarged with increased numbers of organelles; most BS mitochondria are centripetally located

Phase I: Preconditioning

The absence of C_4 photosynthesis in the vast majority of C_3 families indicates that most

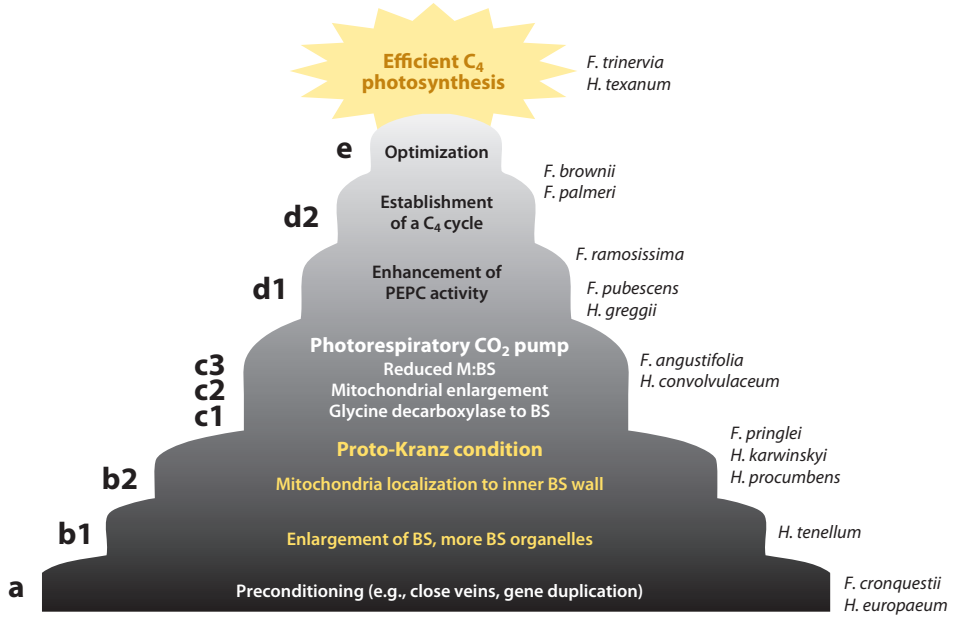

Figure 6

A conceptual model proposing five major phases of C_4 evolution. Important steps within each phase are indicated by numbers. *Flaveria* and *Heliotropium* species corresponding to each stage are shown on the right side. As discussed in the text, the five stages are (*a*) preconditioning; (*b*) the evolution of proto-Kranz anatomy; (*c*) the evolution of C_2 photosynthesis; (*d*) the establishment of the C_4 metabolic cycle with the corresponding localization of the C_3 cycle to the bundle sheath (BS), marking the beginning of C_4 photosynthesis; and (*e*) an optimization phase, in which Kranz anatomy and leaf biochemistry are modified to maximize the efficiency of the C_4 pathway. Additional abbreviations: M, mesophyll; PEPC, PEP carboxylase. Adapted from Reference 117 with permission.

clades have low potential to evolve the C_4 pathway, whereas the clustered distribution of many C_4 lineages indicates a predisposition for C_4 evolution (117, 118). The acquisition of traits that increase the potential for C_4 evolution represents a hypothetical preconditioning phase, the nature of which has remained speculative until recently (117). Clarification

Figure 7

Illustrations demonstrating changes in leaf structure during the evolution of C_4 photosynthesis, based upon *Heliotropium* (99). Abbreviations: BS, bundle sheath; E, epidermis; G, guard cell; GDC, glycine decarboxylase; M, mesophyll; P, palisade parenchyma; S, spongy parenchyma. For clarity, chloroplasts and mitochondria in each panel are shown only for vascular bundles and the middle mesophyll area, and the mesophyll is stylized as having a unifacial palisade parenchyma. C_3 plants typically have small BSs with few organelles, and GDC is expressed in all leaf mitochondria (panel *a*). In the C_3 relatives close to C_4 species (panel *b*), BS cell size increases, forming elongated, bulbous cells with high exposure to intercellular air space. Organelle content is increased in the BS, indicating greater photosynthetic activity of this tissue. GDC remains present in all mitochondria. In proto-Kranz species (panel *c*), BS cells are large and rounded, with abundant organelles. GDC is present in all leaf mitochondria, but most BS mitochondria are localized along the centripetal ends of the BS cells. In C_3–C_4 species employing C_2 photosynthesis (panel *d*), further enlargement of the BS is apparent, while the majority of BS chloroplasts and all BS mitochondria are positioned centripetally. GDC expression has been lost in the M mitochondria. In C_4 plants (panel *e*), BS cells are very large, the number of M cells relative to BS cells is substantially reduced, and all BS chloroplasts and mitochondria are centripetally positioned. BS chloroplasts are enlarged and GDC is expressed only in the BS mitochondria.

a Typical C_3 leaf with high vein density (*H. europaeum*)

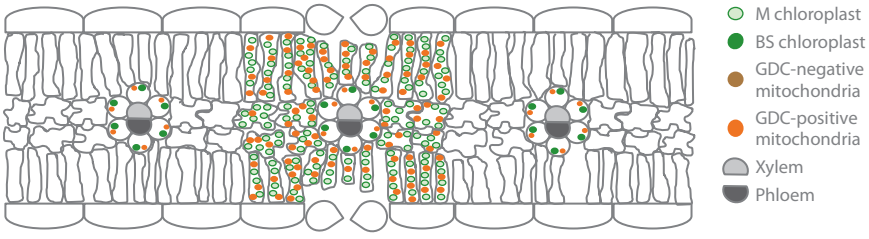

b Leaf of a C_3 plant that is a close relative of the C_4 clade (*H. tenellum*)

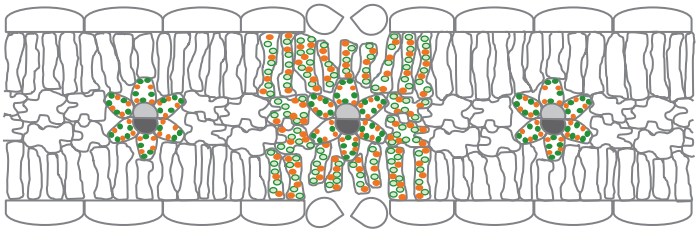

c Proto-Kranz leaf (*H. karwinskyi*)

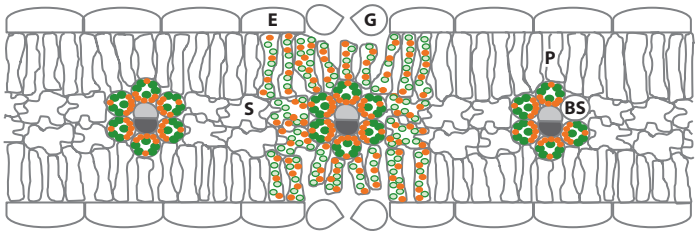

d C_3–C_4 intermediate leaf using C_2 photosynthesis (*H. convolvulaceum*)

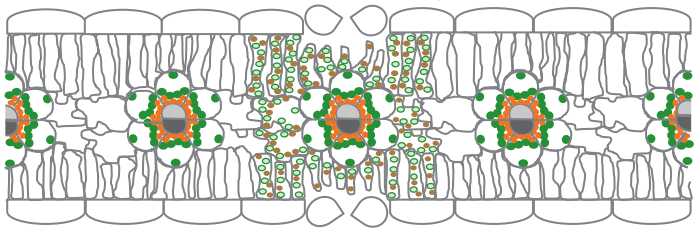

e C_4 leaf (*H. texanum*)

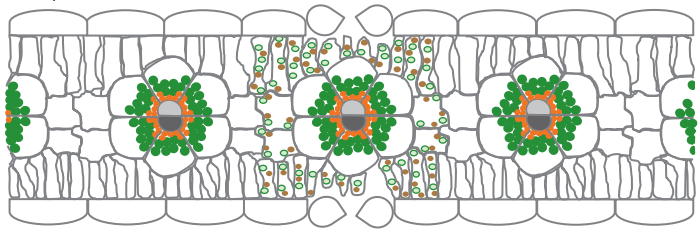

of preconditioning traits has followed the identification of the close C_3 relatives of the C_2 and C_4 nodes within phylogenies.

The best-supported preconditioning trait identified to date is high vein density (i.e., close vein spacing). High vein density has been documented in close C_3 relatives of the C_4 clades in *Cleome*, *Euphorbia*, *Flaveria*, *Heliotropium*, and *Mollugo* (25, 78, 81, 99, 124, 146). In *Euphorbia*, the C_3 species *E. angustifolia* has closer vein spacing than its C_2 sister species *E. acuta* (124), whereas in *Heliotropium* (99) and *Mollugo* (25), the C_3 sister species of the C_4 clades have C_4-like vein spacing. Basal branching C_3 *Cleome* species have vein density similar to that of more distal C_4 *Cleome* species (78, 146). A broad survey of anatomical patterns between 21 closely related C_3 and C_4 species pairs in the eudicots also observed no statistical differences in vein density between the C_3 and C_4 relatives, indicating that the C_3 relatives in the study had already obtained high vein density (98). High vein density in the C_3 progenitors probably results from adaptation to dry climates. Arid-zone angiosperms are noted for high vein density, which is proposed to reduce the path length and resistance for water flow to the sites of evaporation (115, 126, 136). In warm, dry climates, evapotranspiration potential can be very high, necessitating rapid hydraulic flux through the leaves if stomatal closure, loss of turgor, or xylem cavitation are to be avoided (101, 117, 126). For example, an increase in leaf temperature from 25°C to 37°C would quadruple the VPD between leaf and air if the absolute atmospheric humidity were 2 kPa. By reducing vein spacing, the distance between BS and adjacent M cells is reduced, which could then facilitate exchange of metabolites between the M and BS tissues.

Preconditioning may also involve the acquisition of regulatory elements that can easily be modified to confer C_4 patterns of gene expression. In *Flaveria*, an M expression module (MEM) at the distal end of the *ppcA* promoter confers *cis*-regulatory control over the location and intensity of PEPC expression (1, 51). In C_3 *Flaveria* species, the MEM represses expression of PEPC and does not confer cell specificity. During C_4 evolution, the MEM is altered by a modest number of base-pair changes to enhance and localize PEPC expression to the M tissue. Control of the BS-specific expression of NADP-ME and NAD-ME may also be under the control of *trans*-acting regulatory factors that could be modified relatively easily to confer C_4 expression patterns (12).

The other major preconditioning event proposed in the C_3 ancestors is extensive gene duplication and large genome size, which enhances adaptability by providing gene copies that can be neofunctionalized or subfunctionalized without creating harmful mutations (85, 117, 148). Gene duplication is apparent in the origin of C_4-cycle genes for CA, PEPC, PEPCK, NADP-ME, and NADP-malate dehydrogenase (21, 22, 26, 77, 114, 148). A whole-genome duplication event approximately 70 Mya is proposed to have predisposed the grasses to repeatedly evolve C_4 photosynthesis once it was favored by environmental conditions (103, 148). Certain grass lineages, such as Andropogoneae, appear to be rich with duplicated genes from subsequent polyploidy events and single-gene to partial-genome duplications (148).

Phase II: Evolution of Proto-Kranz Anatomy

C_3 species that are closely related to C_2 species have a number of features that indicate the presence of a photorespiratory CO_2 scavenging system within the BS tissue. In *Heliotropium*, C_2 and C_4 photosynthesis occur in section *Orthostachys* (44). In two C_3 species of this section (*H. karwinskyi* and *H. procumbens*), the BS cells are enlarged and have increased organelle numbers relative to other C_3 species within the section (99). The large majority of mitochondria in the BS cells of these species are positioned against the centripetal wall, as commonly observed in C_2 species (99). Some chloroplasts are closely associated with the mitochondria in the centripetal region of the BS cells and contain large starch grains, indicating

they are photosynthetically active. Using an immunolocalization procedure, GDC was shown to be present in both M and BS cells of these *Heliotropium* species, although the centripetal location of the BS mitochondria created a concentrated band of GDC along the inner BS wall (**Figure 7**) (99). Muhaidat et al. (99) termed these features proto-Kranz anatomy because they appear to be incipient versions of Kranz anatomy as found in C_2 and C_4 species. Proto-Kranz features are also apparent in C_3 species of *Diplotaxis*, *Flaveria*, *Neurachne*, and *Steinchisma* that are close to C_2 species in their respective genera. In the C_3 species *F. pringlei* and *Steinchisma laxa* (formerly *Panicum laxum*), mitochondria are more abundant and localized to the centripetal wall of the BS cells, along with a layer of chloroplasts (13, 15; T.L. Sage, unpublished manuscript). In *Diplotaxis viminea*, a C_3 relative of the C_2 species *D. tenuifolia*, numerous mitochondria and chloroplasts are centripetally located in the BS (135). In the C_3 *Neurachne tenuifolia*, the mestome sheath cells are packed with chloroplasts and mitochondria (54).

Muhaidat et al. (99) hypothesized that the proto-Kranz features produce a single-celled glycine shuttle that could scavenge photorespiratory CO_2 produced in the BS tissue and possibly help metabolize an overflow of glycine produced in the M during high photorespiration. With the positioning of mitochondria at the centripetal edge of the cell, glycine produced by photorespiration in centrifugal chloroplasts has to be decarboxylated in the inner region of the cell. Because of the large BS vacuole, the photorespired CO_2 would build up in this region, allowing RuBisCO in the centripetal chloroplasts to operate with higher efficiency. Consistent with this possibility, the photosynthetic CO_2 compensation points of *H. procumbens*, *N. minor*, and *S. laxa* are reduced by 5%–15% relative to C_3 species within their respective genera, indicating recovery of photorespired CO_2 (16, 54, 139). Because the proto-Kranz traits occur in the C_3 relatives of numerous independent lineages of C_2 photosynthesis, it was proposed that evolution of the proto-Kranz anatomy is critical for the initiation of C_4 photosynthesis (99).

The initial events in proto-Kranz evolution appear to be increases in cell size, organelle number, and exposure to intercellular air space of the BS tissue (**Figure 7**). This possibility is supported by anatomical patterns observed in close C_3 relatives of C_2 or proto-Kranz species in *Cleome* (*C. Africana*) (40, 78, 146); *Euphorbia* (*E. angusta*) (124); *Flaveria* (*F. pringlei*) (15; T.L. Sage, unpublished manuscript); *Heliotropium* section *Orthostachys* (*H. tenellum*, *H. calcicola*) (99); C_3 *Mollugo* species (*M. pentaphylla*) (25); and C_3 *Panicum* species that are close to the genus *Steinchisma* (13). In *Heliotropium*, for example, the basal C_3 species in section *Orthostachys* have double the number of chloroplasts in the BS cell than *H. europaeum* of the completely C_3 section *Heliotropium* (99). The functional significance of BS enlargement and increased organelle number in the BS appears to be increased engagement of the BS cell in carbon assimilation. The enlarged BS cells in the above species commonly have enhanced exposure of the outer BS wall to intercellular air spaces, and most of the additional chloroplasts line up along the intercellular air spaces. This is particularly apparent in species that have bulbous BS cells that resemble spongy parenchyma cells, such as *E. angusta*, *H. tenellum*, and *H. calcicola* (99, 124). We hypothesize that the increased engagement of the BS cells in carbon assimilation compensates for the loss of photosynthetic M cells following an increase in vein density.

Phase III: Evolution of C_2 Photosynthesis

The formation of proto-Kranz anatomy is associated with a slight reduction in the CO_2 compensation point of carbon assimilation, indicating modest enhancement of RuBisCO efficiency. Although modest for gas exchange, the proto-Kranz trait could have great significance for C_2 and C_4 evolution because enhanced GDC activity in the BS could allow the leaf to survive a loss of GDC expression in the

M. In this sense, proto-Kranz anatomy would have facilitated the key step in the evolution of C_2 photosynthesis, which is the loss of GDC expression in the M tissue and the consequent establishment of a two-tissue photorespiratory CO_2 loop that concentrates CO_2 into the BS (**Figure 5**) (108). The ubiquity of GDC localization to the BS during C_4 evolution is indicated by phylogenetic branching of C_2 species between C_3 and C_4 nodes in seven distinct lineages of C_4 photosynthesis (**Table 1**). In all cases where intermediate forms have been identified at branch points between C_3 and C_4 lines, C_2 photosynthesis is present, as indicated by mitochondrial localization to the inner BS, immunolocalization of GDC to BS mitochondria, and gas exchange data such as low Γ.

After GDC expression was localized to the BS tissue, the selection pressure would undergo a marked transition: Instead of photorespiration being inhibitory, it would become a resource of CO_2 for the BS chloroplasts. Natural selection might then have favored the optimization of leaf anatomy and physiology to maximize the capture of this internal CO_2 resource. Comparisons within *Flaveria*, *Heliotropium*, and *Steinchisma* indicate that the evolutionary progression from proto-Kranz to fully developed C_2 species involved a further reduction in M cell volume and an increase in BS organelle number (**Figure 7**) (2, 13, 15, 81, 99). Mitochondria, in particular, become larger and more numerous along the inner BS wall, and the chloroplast layer beside the mitochondrial layer is more pronounced (99). The BS cells of C_2 species also form an enlarged, tightly packed sheath that is in close contact with surrounding M cells (13, 78, 81, 99, 124, 146). This restructuring of leaf anatomy creates a version of Kranz anatomy that appears to be optimized for photorespiratory CO_2 concentration because the large BS vacuole slows CO_2 diffusion, and the abundant centripetal chloroplasts would effectively assimilate CO_2 arising from adjacent mitochondria (142). Glycine and serine levels are elevated in leaves employing C_2 photosynthesis, indicating that their movement occurs via diffusion down concentration gradients (90, 109). Together, the changes in vein density, M cell volume, and the size, number, and position of BS organelles establish the structural modifications required for a functional C_4 cycle. By doing so, they facilitate the next phase of C_4 evolution, the upregulation of the C_4 metabolic cycle.

Phase IV: Establishment of the C_4 Metabolic Cycle

C_2 species can be divided into two groups (33). The first group represents C_2 plants in which the reduction in Γ occurs solely through the refixation of photorespired CO_2 in the BS tissue; these have previously been termed type I C_3–C_4 intermediates (33). A second group consists of the type II C_3–C_4 intermediate species, which express limited C_4-cycle activity as indicated by elevated PEPC, pyruvate phosphate dikinase (PPDK), and NADP-ME activities that are roughly 2–5-fold greater than C_3 species and type I intermediates (33, 71, 72, 99). By contrast, C_4 species have PEPC and NADP-ME/NAD-ME activities that are 10–50-fold higher than those of C_3 species (72, 98, 99). Most known type II species occur in *Flaveria* and branch at phylogenetic nodes more distal from the C_3 species than type I intermediates, indicating that engagement of the C_4 cycle follows the establishment of C_2 photosynthesis (33, 82). Type II intermediates have Γ values that are half those of type I intermediates, and up to 55% of their initial CO_2 fixation products are four-carbon acids (72, 89, 90). Type II *Flaveria* species generally lack appreciable activities of PPDK and NADP-ME and thus do not operate a substantial C_4 cycle (71, 72). The main source of PEP in these species is suggested to be the reductive pentose phosphate pathway and glycolysis, which does not have the potential capacity that PPDK would provide (34, 88). They also express RuBisCO at high levels throughout the M (92, 95) and have C_3-like carbon isotope ratios, demonstrating that the C_4 cycle contributes little to overall carbon gain (33, 92, 139).

In the *Flaveria* phylogeny, three C_4-like species (*F. brownii*, *F. palmeri*, *and F. vaginata*)

branch distal to the type II intermediates (82). *F. palmeri* branches between *F. ramosissima* (type II intermediate) and the C_4 *F. campestris*, indicating that it represents an intermediate stage between C_2 and C_4 photosynthesis. *F. vaginata* branches distal to *F. ramosissima* and sister to the C_4 *F. kochiana*. *F. brownii* occurs on a separate branch that includes C_2 species but not C_4 species; it branches in a more distal position from the basal C_3 species than type I C_2 species and is sister to numerous type II species in an unresolved polytomy (82).

As shown by *F. brownii* and *F. palmeri*, C_4-like species conduct C_4 photosynthesis but with some limitations caused by residual expression of M RuBisCO and the use of C_3 forms of key C_4 enzymes (20, 33, 51, 72, 93). This low level of M RuBisCO activity results in a sensitivity of photosynthesis to O_2 reduction (28, 72, 91). Both species operate a fully functional C_4 metabolic cycle with high PEPC, PPDK, and NADP-ME activity (72, 93) and show initial fixation ratios of radiolabeled CO_2 into C_4 acids of over 60%, in contrast to the 50% or less observed in type II species (72, 89, 93). This increase in the initial fixation ratio from <50% to over 60% is proposed to reflect the establishment of an efficient, well-integrated C_4 cycle from the inefficient, poorly coordinated system of the type II intermediates (90, 92). Also, the transition from type II to C_4-like species corresponds to the large reduction in leaf RuBisCO content, acquisition of carbon isotope ratios that approach C_4 values, and an increase in water and nitrogen use efficiencies of photosynthesis from C_3 to C_4 levels at current CO_2 levels (33, 69, 88, 92, 140). The increase in water use efficiency during the transition from C_2 to C_4-like species results from a change in stomatal control from C_3 to C_4 values (60, 140). C_2 species can have higher water use efficiency than C_3 species at low CO_2, but this is due only to increased photosynthesis and not to altered stomatal control, as occurs in C_4-like and C_4 species (33, 88, 140, 141).

In terms of structural changes, *Flaveria linearis* and *F. palmeri* have well-developed Kranz anatomy whereas *F. brownii* has a more intermediate form, with M cells spaced more than one cell distance from the closest BS cell and BS tissue with a less radial appearance than occurs in C_4 *Flaveria* species (15, 81). In the case of *F. brownii*, PEPC activity approaches that of C_4 species; however, it expresses a C_3–C_4 type of PEPC and a C_3 type of CA (38, 72, 77). The C_3-like CA is associated with reduced carboxylation efficiency in *F. brownii* compared with the C_4 *Flaveria* species (28). The regulation of PEPC expression in *F. brownii* is also intermediate between the C_3 and C_4 pattern. PEPC expression in *Flaveria* is controlled by a distal, 41-base-pair region of the *ppcA* promoter named MEM1 (1, 49). Two submodules, A and B, are present in MEM1. In C_4 *Flaveria* species and the C_4-like *F. palmeri*, both the A and B parts are modified to create the enhanced expression and M specificity of the C_4 *ppcA* (1). *Flaveria brownii* has a C_3-like submodule A and a C_4-like submodule B, leading to enhanced expression but weak M specificity (1, 51).

On the basis of the *Flaveria* results, it can be concluded that the acquisition of the full C_4 cycle occurs during the transition from the type II intermediates to the C_4-like species, largely through changes to the promoter elements that enhance expression and compartmentalization of key enzymes such as RuBisCO, PEPC, and CA (1, 38, 51, 77). This can overcome the ineffective coordination apparent in type II intermediates, but does not produce the highly efficient C_4 plants that dominate ecosystems and feed the world. To overcome the deficiencies of the C_4-like condition, a final, fine-tuning phase of C_4 evolution is required to optimize the enzymes, anatomy, and regulatory systems for the C_4 context.

Phase V: Optimization

Highly efficient functioning of C_4 photosynthesis requires close coordination of the C_3 and C_4 cycles, altered regulation and kinetics of C_4-cycle enzymes to operate in novel cellular environments, close association of M and BS tissues to minimize diffusion distances, and

effective integration of the C_4 pathway into the physiology of the entire plant (57, 117). As demonstrated by comparisons between C_4-like and C_4 *Flaveria* species, many of the evolutionary changes that optimize regulatory and kinetic properties of C_4 enzymes occur late in the evolution of the C_4 pathway. Evolution of C_4 PEPC clearly illustrates this point. In C_4 plants, the C_4-type PEPC has reduced sensitivity to malate and a lower K_m for PEP compared with C_3 isoforms (1, 21, 51). High malate concentrations are present in C_4 leaves and are necessary for its rapid diffusion into the BS; however, malate is an inhibitor of PEPC, so to compensate, the malate sensitivity of PEPC has to be reduced. This is accomplished by changes in PEPC regions 2 and 5 in C_4 *Flaveria* species (51, 62). In region 2, 16 amino acid residues differ between the C_3 and C_4 forms of PEPC; of these, only 1 is shared by the C_4 PEPCs of *F. brownii* and the C_4 *F. trinervia*. Much of the change in K_m (PEP) occurs via a substitution at position 774 of PEPC (9, 38, 51): In all C_2 *Flaveria* species and *F. brownii*, this position is an alanine, whereas in all C_4 plants it is a serine. In *Mollugo*, after the C_4 pathway evolved, the distinct branches of the C_4 species *M. cerviana* independently evolved the C_4-type PEPC (as indicated by the separate acquisition of the serine at position 774) as well as four other amino acids at sites known to confer C_4 properties to PEPC (25). C_3–C_4 *Alternanthera* species also lack the C_4-type PEPC found in C_4 *Alternanthera* species (50). These cases provide multiple independent examples that the C_4 isoform of PEPC appears late in C_4 evolution, after the establishment of the C_4 metabolic cycle.

The acquisition of the C_4 form of RuBisCO also occurs after the C_4 cycle has been assembled. During C_4 evolution in *Flaveria*, RuBisCO evolved from a C_3 type with relatively low k_{cat} and K_c values to a C_4 type with high k_{cat} and K_c values (73). These changes are primarily associated with two amino acid substitutions on the large subunit at positions 309 and 149 that are present in all of the C_4 *Flaveria* species examined (66). The substitutions at positions 309 and 149 are absent in the C_3 species, and only one is present in the C_4-like *F. palmeri* (66). *Flaveria brownii* expresses a RuBisCO with C_3-like k_{cat} and K_c values, indicating that it lacks both of the amino acid substitutions of the C_4 isoform (73). Additional work is needed to confirm this possibility.

SYNTHESIS AND CONCLUSION

In the past half decade, there has been a convergence of molecular, physiological, structural, and paleoecological data that provides a detailed understanding of how, when, and where C_4 photosynthesis was able to evolve. Multiple lines of complementary evidence now point to high rates of photorespiration as the principal driver of C_4 evolution. Geological and molecular clock studies indicate that C_4 lineages evolved after Earth's atmospheric CO_2 concentration declined to levels causing high rates of photorespiration in warm climates. The species that branch on the phylogeny closest to the C_4 lineages are consistently found in environments that are hot, of low humidity, and somewhat barren owing to disturbance or abiotic stress. These environments indicate that drought or elevated salinity were common, but in all cases, episodic summer rains would have allowed for photosynthetic activity and high rates of photorespiration during the hot summer months. High photorespiration would inhibit the C_3 competition, but more importantly, it would provide a valuable resource—internally released CO_2—that could be concentrated to boost the efficiency of RuBisCO. Evolutionary exploitation of photorespired CO_2 best explains the stepwise assembly of C_4 photosynthesis, with each step facilitating subsequent steps. Hot, dry environments promoted high vein density, which in turn facilitated greater photosynthetic activity in the BS tissue, possibly to offset the loss of M tissue. Photosynthetically active BS cells then evolved proto-Kranz anatomy by repositioning mitochondria to the inner region of enlarged BS cells. This would have enabled the survival of a mutation that knocked out GDC expression in the M tissue,

thus creating the two-celled photorespiratory cycle that concentrates CO_2 into the BS. Natural selection then established C_2 photosynthesis to efficiently trap and refix this CO_2, and in the process, created the basic version of the Kranz anatomy that is essential to most forms of C_4 photosynthesis. Once the Kranz features were in place, the activity of PEPC and other C_4-cycle enzymes were upregulated, eventually creating a fully functional C_4 cycle. Following the reduction of RuBisCO and the C_3 cycle in the M tissue, C_4 photosynthesis was born, although in an inefficient state. With further adjustments to optimize the C_4 cycle, productive, highly competitive C_4 plants evolved and radiated over the countryside.

The large number of C_4 lineages provides hope that C_4 photosynthesis would be easy to engineer into C_3 crops, and that the C_4 evolutionary trajectories observed in nature may provide directions for improving crop productivity. Strategies to engineer the C_4 pathway into C_3 crops need not mimic the pathway of C_4 evolution, however, as the intervening stage of C_2 photosynthesis represents a distinct CO_2-concentrating mechanism with its own optimal state. Although photorespiration might be the bridge to C_4 photosynthesis, it is also a constraint, in that more direct routes could have been precluded by the need to first establish a C_2-type CO_2-concentrating system. Humans do not have this constraint. Instead of following the path of C_4 evolution, humans can mine the genetic resources within the many lineages of C_4 plants to identify the critical genetic elements needed for C_4 photosynthesis. With the advent of high-throughput technologies, genome comparisons between the close C_2, C_3, and C_4 species should be able to quickly identify the key factors controlling C_4 expression. With these tools, humans should thus be able to introduce the C_4 syndrome into a C_3 crop in a relative instant in evolutionary time.

SUMMARY POINTS

1. At least 66 distinct evolutionary lineages of C_4 photosynthesis have been identified; all are angiosperms. These lineages tend to be clustered in the angiosperm phylogeny, with most arising in groups from hot environments with a high potential for evapotranspiration.
2. C_4 photosynthesis evolved as a response to high rates of photorespiration that were promoted by a decline in atmospheric CO_2 over the past 40 million years. High temperature, and in many cases drought or salinity, interacted with low CO_2 to promote high rates of photorespiration.
3. The evolutionary progression from C_3 to C_4 photosynthesis involves a series of characteristic stages. Two important stages are the formation of proto-Kranz anatomy in close C_3 relatives of C_4 species and the formation of a C_2 photosynthetic mechanism in C_3–C_4 intermediate species.
4. The initiation of C_4 evolution is hypothesized to be facilitated by high vein density in leaves adapted to high evapotranspiration. High vein density may promote the formation of enlarged BS cells, which in turn may lead to enhanced organelle numbers in the BS and localization of mitochondria to the inner edge of the BS cells. These traits collectively make up the proto-Kranz syndrome, which may function to scavenge photorespired CO_2 produced in the bundle sheath.

5. The formation of C_2 photosynthesis follows a loss of GDC expression in the M tissue such that BS GDC must metabolize all the photorespiratory products in the leaf. Elaboration of this mechanism to efficiently recapture photorespired CO_2 leads to Kranz anatomy. The formation of Kranz anatomy facilitates the upregulation of a C_4 metabolic cycle.

FUTURE ISSUES

1. Increasing phylogenetic detail should improve the ability to identify C_3–C_4 intermediate species and their close C_3 relatives in many additional lineages of C_4 evolution. This will assist comparative approaches designed to test hypotheses of C_4 evolution.
2. The adaptive function of high vein density in C_3 relatives of C_4 lineages remains to be identified.
3. The function of centripetal positioning of mitochondria in proto-Kranz species remains to be identified.
4. The genes controlling the evolutionary transitions remain to be identified. Comparative genomic approaches should be able to identify the genetic changes along the phylogenetic gradient, which would assist efforts to engineer the C_4 pathway into C_3 crops.

DISCLOSURE STATEMENT

The authors are not aware of any affiliations, memberships, funding, or financial holdings that might be perceived as affecting the objectivity of this review.

ACKNOWLEDGMENTS

We acknowledge the assistance of Professor Erika Edwards, who supplied **Figure 2**, and the financial support of the National Science and Engineering Research Council of Canada to R.F.S. and T.L.S.

LITERATURE CITED

1. Akyildiz M, Gowik U, Engelmann S, Koczor M, Streubel M, Westhoff P. 2007. Evolution and function of a *cis*-regulatory module for mesophyll-specific gene expression in the C_4 dicot *Flaveria trinervia*. *Plant Cell* 19:3391–402
2. Aliscioni SS, Giussani LM, Zuloaga FO, Kellogg EA. 2003. A molecular phylogeny of *Panicum* (Poaceae: Paniceae): tests of monophyly and phylogenetic placement within the Panicoideae. *Am. J. Bot.* 90:796–821
3. Arakaki M, Christin PA, Nyffeler R, Lendel A, Eggli U, et al. 2011. Contemporaneous and recent radiations of the world's major succulent plant lineages. *Proc. Natl. Acad. Sci. USA* 108:8379–84
4. Bauwe H. 2011. Photorespiration: the bridge to C_4 photosynthesis. See Ref. 106, pp. 81–108
5. Bauwe H, Keerberg O, Bassuner R, Parnik T, Bassuner B. 1987. Reassimilation of carbon-dioxide by *Flaveria* (Asteraceae) species representing different types of photosynthesis. *Planta* 172:214–18
6. Beerling DJ, Osborne CP. 2006. The origin of the savanna biome. *Glob. Change Biol.* 12:2023–31
7. Beerling DJ, Royer DL. 2011. Convergent Cenozoic CO_2 history. *Nat. Geosci.* 4:418–20

8. Besnard G, Muasya AM, Russier F, Roalson EH, Salamin N, Christin PA. 2009. Phylogenomics of C_4 photosynthesis in sedges (Cyperaceae): multiple appearances and genetic convergence. *Mol. Biol. Evol.* 26:1909–19
9. Blasing OE, Westhoff P, Svensson P. 2000. Evolution of C_4 phosphoenolpyruvate carboxylase in *Flaveria*, a conserved serine residue in the carboxyl-terminal part of the enzyme is a major determinant for C_4-specific characteristics. *J. Biol. Chem.* 275:27917–23
10. Bobe R, Behrensmeyer AK. 2004. The expansion of grassland ecosystems in Africa in relation to mammalian evolution and the origin of the genus *Homo*. *Palaeogeogr. Palaeoclimatol. Palaeoecol.* 207:399–420
11. Bouchenak-Khelladi Y, Verboom GA, Hodkinson TR, Salamin N, Francois O, et al. 2009. The origins and diversification of C_4 grasses and savanna-adapted ungulates. *Glob. Change Biol.* 15:2397–417
12. Brown NJ, Newell CA, Stanley S, Chen JE, Perrin AJ, et al. 2011. Independent and parallel recruitment of preexisting mechanisms underlying C_4 photosynthesis. *Science* 331:1436–39
13. Brown RH, Bouton JH, Rigsby L, Rigler M. 1983. Photosynthesis of grass species differing in carbon-dioxide fixation pathways. VIII. Ultrastructural characteristics of *Panicum* species in the *Laxa* group. *Plant Physiol.* 71:425–31
14. Brown RH, Byrd GT, Black CC. 1991. Assessing the degree of C_4 photosynthesis in C_3-C_4 species using an inhibitor of phospho*enol*pyruvate carboxylase. *Plant Physiol.* 97:985–89
15. Brown RH, Hattersley PW. 1989. Leaf anatomy of C_3-C_4 species as related to evolution of C_4 photosynthesis. *Plant Physiol.* 91:1543–50
16. Brown RH, Morgan JA. 1980. Photosynthesis of grass species differing in carbon-dioxide fixation pathways. 6. Differential-effects of temperature and light-intensity on photo-respiration in C_3, C_4 and intermediate species. *Plant Physiol.* 66:541–44
17. Campbell CD, Sage RF, Kocacinar F, Way DA. 2005. Estimation of the whole-plant CO_2 compensation point of tobacco (*Nicotiana tabacum* L.). *Glob. Change Biol.* 11:1956–67
18. Cerling TE. 1999. Paleorecords of C_4 plants and ecosystems. See Ref. 121, pp. 445–69
19. Cerling TE, Harris JM, MacFadden BJ, Leakey MG, Quade J, et al. 1997. Global vegetation change through the Miocene/Pliocene boundary. *Nature* 389:153–58
20. Cheng SH, Moore BD, Edwards GE, Ku MSB. 1988. Photosynthesis in *Flaveria brownii*, a C_4-like species-leaf anatomy, characteristics of CO_2 exchange, compartmentation of photosynthetic enzymes and metabolism of (CO_2)-C^{14}. *Plant Physiol.* 87:867–73
21. Christin P-A, Salamin N, Savolainen V, Duvall MR, Besnard G. 2007. C_4 photosynthesis evolved in grasses via parallel adaptive genetic changes. *Curr. Biol.* 17:1241–47
22. Christin PA, Besnard G. 2009. Two independent C_4 origins in Aristidoideae (Poaceae) revealed by the recruitment of distinct phosphoenolpyruvate carboxylase genes. *Am. J. Bot.* 96:2234–39
23. Christin PA, Besnard G, Samaritani E, Duvall MR, Hodkinson TR, et al. 2008. Oligocene CO_2 decline promoted C_4 photosynthesis in grasses. *Curr. Biol.* 18:37–43
24. Christin PA, Osborne CP, Sage RF, Arakaki M, Edwards EJ. 2011. C_4 eudicots are not younger than C_4 monocots. *J. Exp. Bot.* 62:3171–81
25. Christin PA, Sage TL, Edwards EJ, Ogburn RM, Khoshravesh R, Sage RF. 2011. Complex evolutionary transitions and the significance of C_3-C_4 intermediate forms of photosynthesis in Molluginaceae. *Evolution* 65:643–60
26. Christin PA, Salamin N, Kellogg EA, Vicentini A, Besnard G. 2009. Integrating phylogeny into studies of C_4 variation in the grasses. *Plant Physiol.* 149:82–87
27. Cowling SA, Sage RF. 1998. Interactive effects of low atmospheric CO_2 and elevated temperature on growth, photosynthesis and respiration in *Phaseolus vulgaris*. *Plant Cell Environ.* 21:427–35
28. Dai ZY, Ku MSB, Edwards GE. 1996. Oxygen sensitivity of photosynthesis and photorespiration in different photosynthetic types in the genus *Flaveria*. *Planta* 198:563–71
29. Dengler NG, Nelson T. 1999. Leaf structure and development in C_4 plants. See Ref. 121, pp. 133–72
30. Devi MT, Rajagopalan AV, Raghavendra AS. 1995. Predominant localization of mitochondria enriched with glycine-decarboxylating enzymes in bundle-sheath cells of *Alternanthera tenella*, a C_3-C_4 intermediate species. *Plant Cell Environ.* 18:589–94
31. Edwards EJ, Osborne CP, Stromberg CAE, Smith SA, C_4 Grasses Consort. 2010. The origins of C_4 grasslands: integrating evolutionary and ecosystem science. *Science* 328:587–91

23. The first comprehensive estimate of when C_4 lineages first appeared; see also Ref. 138, which was published a few months later.

31. A concise yet informative analysis of the rise of C_4 grasses and grasslands.

32. Edwards EJ, Smith SA. 2010. Phylogenetic analyses reveal the shady history of C_4 grasses. *Proc. Natl. Acad. Sci. USA* 107:2532–37
33. Edwards GE, Ku MSB. 1987. Biochemistry of C_3-C_4 intermediates. In *The Biochemistry of Plants*, Vol. 10: *Photosynthesis*, ed. MD Hatch, NK Boardman, pp. 275–325. New York: Academic
34. Edwards GE, Ku MSB, Hatch MD. 1982. Photosynthesis in *Panicum milioides*, a species with reduced photo-respiration. *Plant Cell Physiol.* 23:1185–95
35. Edwards GE, Voznesenskya EV. 2011. C_4 photosynthesis: kranz forms and single-cell C_4 in terrestrial plants. See Ref. 106, pp. 29–61
36. Ehleringer JR, Cerling TE, Helliker BR. 1997. C_4 photosynthesis, atmospheric CO_2 and climate. *Oecologia* 112:285–99
37. **Ehleringer JR, Sage RF, Flanagan LB, Pearcy RW. 1991. Climate change and the evolution of C_4 photosynthesis. *Trends Ecol. Evol.* 6:95–99**
38. Engelmann S, Blasing OE, Gowik U, Svensson P, Westhoff P. 2003. Molecular evolution of C_4 phosphoenolpyruvate carboxylase in the genus *Flaveria*—a gradual increase from C_3 to C_4 characteristics. *Planta* 217:717–25
39. Engelmann S, Wiludda C, Burscheidt J, Gowik U, Schlue U, et al. 2008. The gene for the P-subunit of glycine decarboxylase from the C_4 species *Flaveria trinervia*: analysis of transcriptional control in transgenic *Flaveria bidentis* C_4 and *Arabidopsis* C_3. *Plant Physiol.* 146:1773–85
40. Feodorova TA, Voznesenskaya EV, Edwards GE, Roalson EH. 2010. Biogeographic patterns of diversification and the origins of C_4 in *Cleome* (Cleomaceae). *Syst. Bot.* 35:811–26
41. Fox DL, Koch PL. 2003. Tertiary history of C_4 biomass in the Great Plains, USA. *Geology* 31:809–12
42. Fox DL, Koch PL. 2004. Carbon and oxygen isotopic variability in Neogene paleosol carbonates: constraints on the evolution of the C_4-grasslands of the Great Plains, USA. *Palaeogeogr. Palaeoclimatol. Palaeoecol.* 207:305–29
43. Franks PJ, Beerling DJ. 2009. Maximum leaf conductance driven by CO_2 effects on stomatal size and density over geologic time. *Proc. Natl. Acad. Sci. USA* 106:10343–47
44. Frohlich M. 1978. *Systematics of* Heliotropium *section* Orthostachys *in Mexico*. PhD thesis. Harvard Univ.
45. Furbank RT. 2011. Evolution of the C_4 photosynthetic mechanism: Are there really three C_4 acid decarboxylation types? *J. Exp. Bot.* 62: 3103–8
46. Gaut BS, Doebley JF. 1997. DNA sequence evidence for the segmental allotetraploid origin of maize. *Proc. Natl. Acad. Sci. USA* 94:6809–14
47. Gelin Z, Mosyakin SL, Clements SE. 2003. Chenopodiaceae. In *Flora of China*, *Ulmaceae Through Basellaceae*, ed. W Zhengyi, PH Raven, H Deyuan, pp. 351–414. St. Louis: Mo. Bot. Gard.
48. Gerhart LM, Ward JK. 2010. Plant responses to low [CO_2] of the past. *New Phytol.* 188:674–95
49. Gowik U, Burscheidt J, Akyildiz M, Schlue U, Koczor M, et al. 2004. *cis*-Regulatory elements for mesophyll-specific gene expression in the C_4 plant *Flaveria trinervia*, the promoter of the C_4 phosphoenolpyruvate carboxylase gene. *Plant Cell* 16:1077–90
50. Gowik U, Engelmann S, Blasing OE, Raghavendra AS, Westhoff P. 2006. Evolution of C_4 phosphoenolpyruvate carboxylase in the genus *Alternanthera*: gene families and the enzymatic characteristics of the C_4 isozyme and its orthologues in C_3 and C_3/C_4 *Alternantheras*. *Planta* 223:359–68
51. Gowik U, Westhoff P. 2011. C_4-phosphoenolpyruvate carboxylase. See Ref. 106, pp. 257–75
52. Grass Phylogeny Work. Group II. 2012. New grass phylogeny resolves deep evolutionary relationships and discovers C_4 origins. *New Phytol.* 193:304–12
53. Hatch MD. 1987. C_4 photosynthesis: a unique blend of modified biochemistry, anatomy and ultrastructure. *Biochim. Biophys. Acta* 895:81–106
54. Hattersley PW, Wong SC, Perry S, Roksandic Z. 1986. Comparative ultrastructure and gas-exchange characteristics of the C_3-C_4 intermediate *Neurachne minor* S. T. Blake (Poaceae). *Plant Cell Environ.* 9:217–33
55. Haupt-Herting S, Klug K, Fock HP. 2001. A new approach to measure gross CO_2 fluxes in leaves. Gross CO_2 assimilation, photorespiration, and mitochondrial respiration in the light in tomato under drought stress. *Plant Physiol.* 126:388–96
56. Hedge BA, Patil TM. 1980. Physiological studies on *Parthenium hysterophorus* under different ecological conditions. *Biovigyanam* 6:15–20

37. The first presentation of the CO_2 starvation hypothesis for C_4 evolution. The arguments are still valid, although the timing has since been revised.

57. Hibberd JM, Covshoff S. 2010. The regulation of gene expression required for C_4 photosynthesis. *Annu. Rev. Plant Biol.* 62:181–207
58. Holaday AS, Lee KW, Chollet R. 1984. C_3-C_4 intermediate species in the genus *Flaveria*: leaf anatomy, ultrastructure, and the effect of O_2 on the CO_2 compensation concentration. *Planta* 160:25–32
59. Huber M, Caballero R. 2011. The early Eocene equable climate problem revisited. *Clim. Past* 7:603–33
60. Huxman TE, Monson RK. 2003. Stomatal responses of C_3, C_3-C_4 and C_4 *Flaveria* species to light and intercellular CO_2 concentration: implications for the evolution of stomatal behaviour. *Plant Cell Environ.* 26:313–22
61. Hylton CM, Rawsthorne S, Smith AM, Jones DA, Woolhouse HW. 1988. Glycine decarboxylase is confined to the bundle-sheath cells of leaves of C_3-C_4 intermediate species. *Planta* 175:452–59
62. Jacobs B, Engelmann S, Westhoff P, Gowik U. 2008. Evolution of C_4 phosphoenolpyruvate carboxylase in *Flaveria*: determinants for high tolerance towards the inhibitor L-malate. *Plant Cell Environ.* 31:793–803
63. Jordan DB, Ogren WL. 1984. The CO_2/O_2 specificity of ribulose 1,5-bisphosphate carboxylase oxygenase: dependence on ribulosebisphosphate concentration, pH and temperature. *Planta* 161:308–13
64. Kadereit G, Freitag H. 2011. Molecular phylogeny of Camphorosmeae (Camphorosmoideae, Chenopodiaceae): implications for biogeography, evolution of C_4-photosynthesis and taxonomy. *Taxon* 60:51–78
65. Kanai R, Edwards EJ. 1999. The biochemistry of C_4 photosynthesis. See Ref. 121, pp. 49–87
66. Kapralov MV, Kubien DS, Andersson I, Filatov DA. 2011. Changes in Rubisco kinetics during the evolution of C_4 photosynthesis in *Flaveria* (Asteraceae) are associated with positive selection on genes encoding the enzyme. *Mol. Biol. Evol.* 28:1491–503
67. Keeley JE, Rundel PW. 2005. Fire and the Miocene expansion of C_4 grasslands. *Ecol. Lett.* 8:683–90
68. Kellogg EA. 1999. Phylogenetic aspects of the evolution of C_4 photosynthesis. See Ref. 121, pp. 411–44
69. Kocacinar F, McKown AD, Sage TL, Sage RF. 2008. Photosynthetic pathway influences xylem structure and function in *Flaveria* (Asteraceae). *Plant Cell Environ.* 31:1363–76
70. Koteyeva NK, Voznesenskaya EV, Berry JO, Chuong SDX, Franceschi VR, Edwards GE. 2011. Development of structural and biochemical characteristics of C_4 photosynthesis in two types of Kranz anatomy in genus *Suaeda* (family Chenopodiaceae). *J. Exp. Bot.* 62:3197–212
71. Ku MSB, Monson RK, Littlejohn RO, Nakamoto H, Fisher DB, Edwards GE. 1983. Photosynthetic characteristics of C_3-C_4 intermediate *Flaveria* species: I. Leaf anatomy, photosynthetic responses to O_2 and CO_2, and activities of key enzymes in the C_3 and C_4 pathways. *Plant Physiol.* 71:944–48
72. Ku MSB, Wu JR, Dai ZY, Scott RA, Chu C, Edwards GE. 1991. Photosynthetic and photorespiratory characteristics of *Flaveria* species. *Plant Physiol.* 96:518–28
73. Kubien DS, Whitney SM, Moore PV, Jesson LK. 2008. The biochemistry of Rubisco in *Flaveria*. *J. Exp. Bot.* 59:1767–77
74. Kurschner WM, Kvacek Z, Dilcher DL. 2008. The impact of Miocene atmospheric carbon dioxide fluctuations on climate and the evolution of terrestrial ecosystems. *Proc. Natl. Acad. Sci. USA* 105:449–53
75. Kuypers MMM, Pancost RD, Damste JSS. 1999. A large and abrupt fall in atmospheric CO_2 concentration during Cretaceous times. *Nature* 399:342–45
76. Loreto F, Delfine S, Di Marco G. 1999. Estimation of photorespiratory carbon dioxide recycling during photosynthesis. *Aust. J. Plant Physiol.* 26:733–36
77. Ludwig M. 2011. The molecular evolution of β-carbonic anhydrase in *Flaveria*. *J. Exp. Bot.* 62:3071–81
78. Marshall DM, Muhaidat R, Brown NJ, Liu Z, Stanley S, et al. 2007. *Cleome*, a genus closely related to *Arabidopsis*, contains species spanning a developmental progression from C_3 to C_4 photosynthesis. *Plant J.* 51:886–96
79. McElwain JC, Willis KJ, Lupia R. 2005. Cretaceous CO_2 decline and the radiation and diversification of angiosperms. In *A History of Atmospheric CO_2 and Its Effects on Plants, Animals, and Ecosystems*, ed. JR Ehleringer, TE Cerling, MD Dearing, pp. 133–65. New York: Springer
80. McInerney FA, Stromberg CAE, White JWC. 2011. The Neogene transition from C_3 to C_4 grasslands in North America: stable carbon isotope ratios of fossil phytoliths. *Paleobiology* 37:23–49

81. McKown AD, Dengler NG. 2007. Key innovations in the evolution of Kranz anatomy and C_4 vein pattern in *Flaveria* (Asteraceae). *Am. J. Bot.* 94:382–99

82. A comprehensive, species-level phylogeny of the model genus used for the study of C_4 evolution.

82. McKown AD, Moncalvo JM, Dengler NG. 2005. Phylogeny of *Flaveria* (Asteraceae) and inference of C_4 photosynthesis evolution. *Am. J. Bot.* 92:1911–28

83. Mo. Bot. Gard. 2011. Tropicos. **http://www.tropicos.org**

84. Monson RK. 1999. The origins of C_4 genes and evolutionary pattern in the C_4 metabolic phenotype. See Ref. 121, pp. 337–410

85. Monson RK. 2003. Gene duplication, neofunctionalization, and the evolution of C_4 photosynthesis. *Int. J. Plant Sci.* 164:S43–54

86. The first paper to propose that glycine shuttling is a critical step in the evolution of C_4 photosynthesis.

86. Monson RK, Edwards GE, Ku MSB. 1984. C_3-C_4 intermediate photosynthesis in plants. *BioScience* 34:563–66, 571–74

87. Monson RK, Jaeger CH. 1991. Photosynthetic characteristics of C_3-C_4 intermediate *Flaveria floridana* (Asteraceae) in natural habitats: evidence of advantages to C_3-C_4 photosynthesis at high leaf temperatures. *Am. J. Bot.* 78:795–800

88. Monson RK, Moore BD. 1989. On the significance of C_3-C_4 intermediate photosynthesis to the evolution of C_4 photosynthesis. *Plant Cell Environ.* 12:689–99

89. Monson RK, Moore BD, Ku MSB, Edwards GE. 1986. Co-function of C_3 photosynthetic and C_4 photosynthetic pathways in C_3, C_4 and C_3-C_4 intermediate *Flaveria* species. *Planta* 168:493–502

90. The most comprehensive review of C_3–C_4 intermediacy published to date.

90. Monson RK, Rawsthorne S. 2000. Carbon dioxide assimilation in C_3-C_4 intermediate plants. In *Photosynthesis: Physiology and Metabolism*, ed. RC Leegood, TD Sharkey, S Von Caemmerer, pp. 533–50. Dordrecht: Kluwer Acad.

91. Monson RK, Schuster WS, Ku MSB. 1987. Photosynthesis in *Flaveria brownii* A.M. Powell: a C_4-like C_3-C_4 intermediate. *Plant Physiol.* 85:1063–67

92. Monson RK, Teeri JA, Ku MSB, Gurevitch J, Mets LJ, Dudley S. 1988. Carbon-isotope discrimination by leaves of *Flaveria* species exhibiting different amounts of C_3-cycle and C_4-cycle co-function. *Planta* 174:145–51

93. Moore BD, Edwards GE. 1989. Metabolism of $^{14}CO_2$ by leaves of different photosynthetic types of *Neurachne* species. *Plant Sci.* 60:155–61

94. Moore BD, Franceschi VR, Cheng SH, Wu JR, Ku MSB. 1987. Photosynthetic characteristics of the C_3-C_4 intermediate *Parthenium hysterophorus*. *Plant Physiol.* 85:978–83

95. Moore BD, Monson RK, Ku MSB, Edwards GE. 1988. Activities of principal photosynthetic and photorespiratory enzymes in leaf mesophyll and bundle sheath protoplasts from the C_3-C_4 intermediate *Flaveria ramosissima*. *Plant Cell Physiol.* 29:999–1006

96. Moore PD. 1983. Plants and the palaeoatmosphere. *J. Geol. Soc.* 140:13–25

97. Morgan CL, Turner SR, Rawsthorne S. 1993. Coordination of the cell-specific distribution of the 4 subunits of glycine decarboxylase and of serine hydroxymethyltransferase in leaves of C_3-C_4 intermediate species from different genera. *Planta* 190:468–73

98. Muhaidat R, Sage RF, Dengler NG. 2007. Diversity of Kranz anatomy and biochemistry in C_4 eudicots. *Am. J. Bot.* 94:362–81

99. Muhaidat R, Sage TL, Frohlich MW, Dengler NG, Sage RF. 2011. Characterization of C_3-C_4 intermediate species in the genus *Heliotropium* L. (Boraginaceae): anatomy, ultrastructure and enzyme activity. *Plant Cell Environ.* 34:1723–36

100. Osborne CP, Freckleton RP. 2009. Ecological selection pressures for C_4 photosynthesis in the grasses. *Proc. R. Soc. B* 276:1753–60

101. Osborne CP, Sack L. 2012. Evolution of C_4 plants: a new hypothesis for an interaction of CO_2 and water relations mediated by plant hydraulics. *Philos. Trans. R. Soc. B.* 367:583–600

102. Parnik T, Keerberg O. 2007. Advanced radiogasometric method for the determination of the rates of photorespiratory and respiratory decarboxylations of primary and stored photosynthates under steady-state photosynthesis. *Physiol. Plant.* 129:34–44

103. Paterson AH, Bowers JE, Chapman BA. 2004. Ancient polyploidization predating divergence of the cereals, and its consequences for comparative genomics. *Proc. Natl. Acad. Sci. USA* 101:9903–8

104. Powell AM. 1978. Systematics of *Flaveria* (Flaveriinae Asteraceae). *Ann. Mo. Bot. Gard.* 65:590–636

105. Prendergast HDV, Hattersley PW. 1985. Distribution and cytology of Australian *Neurachne* and its allies (Poaceae), a group containing C_3, C_4 and C_3-C_4 intermediate species. *Aust. J. Bot.* 33:317–36

106. Raghavendra AS, Sage RF. 2011. *C_4 Photosynthesis and Related CO_2 Concentrating Mechanisms*. Dordrecht: Springer

107. Rajendrudu G, Prasad JSR, Das VSR. 1986. C_3-C_4 intermediate species in *Alternanthera* (Amaranthaceae): leaf anatomy, CO_2 compensation point, net CO_2 exchange and activities of photosynthetic enzymes. *Plant Physiol.* 80:409–14

108. Rawsthorne S. 1992. C_3-C_4 intermediate photosynthesis: linking physiology to gene-expression. *Plant J.* 2:267–74

109. Rawsthorne S, Hylton CM. 1991. The relationship between the post-illumination CO_2 burst and glycine metabolism in leaves of C_3 and C_3-C_4 intermediate species of *Moricandia*. *Planta* 186:122–26

110. Rawsthorne S, Hylton CM, Smith AM, Woolhouse HW. 1988. Distribution of photorespiratory enzymes between bundle-sheath and mesophyll-cells in leaves of the C_3-C_4 intermediate species *Moricandia arvensis* (L.) DC. *Planta* 176:527–32

111. Rawsthorne S, Hylton CM, Smith AM, Woolhouse HW. 1988. Photorespiratory metabolism and immunogold localization of photorespiratory enzymes in leaves of C_3 and C_3-C_4 intermediate species of *Moricandia*. *Planta* 173:298–308

112. Roalson EH, Hinchliff CE, Trevisan R, da Silva CRM. 2010. Phylogenetic relationships in *Eleocharis* (Cyperaceae): C_4 photosynthesis origins and patterns of diversification in the spikerushes. *Syst. Bot.* 35:257–71

113. Roessler PG, Monson RK. 1985. Midday depression in net photosynthesis and stomatal conductance in *Yucca glauca*: relative contributions of leaf temperature and leaf-to-air water-vapor concentration difference. *Oecologia* 67:380–87

114. Rondeau P, Rouch C, Besnard G. 2005. NADP-malate dehydrogenase gene evolution in Andropogoneae (Poaceae): gene duplication followed by sub-functionalization. *Ann. Bot.* 96:1307–14

115. Roth-Nebelsick A, Uhl D, Mosbrugger V, Kerp H. 2001. Evolution and function of leaf venation architecture: a review. *Ann. Bot.* 87:553–66

116. Sage RF. 2001. Environmental and evolutionary preconditions for the origin and diversification of the C_4 photosynthetic syndrome. *Plant Biol.* 3:202–13

117. Sage RF. 2004. The evolution of C_4 photosynthesis. *New Phytol.* 161:341–70

118. Sage RF, Christin PA, Edwards EJ. 2011. The C_4 plant lineages of planet Earth. *J. Exp. Bot.* 62:3155–69

119. Sage RF, Coleman JR. 2001. Effects of low atmospheric CO_2 on plants: more than a thing of the past. *Trends Plant Sci.* 6:18–24

120. Sage RF, Li M, Monson RK. 1999. The taxonomic distribution of C_4 photosynthesis. See Ref. 121, pp. 551–85

121. Sage RF, Monson RK. 1999. *C_4 Plant Biology*. San Diego: Academic

122. Sage RF, Sage TL, Pearcy RW, Borsch T. 2007. The taxonomic distribution of C_4 photosynthesis in Amaranthaceae *sensu stricto*. *Am. J. Bot.* 94:1992–2003

123. Sage TL, Sage RF. 2009. The functional anatomy of rice leaves: implications for refixation of photorespiratory CO_2 and efforts to engineer C_4 photosynthesis into rice. *Plant Cell Physiol.* 50:756–72

124. Sage TL, Sage RF, Vogan PJ, Rahman B, Johnson DC, et al. 2011. The occurrence of C_2 photosynthesis in *Euphorbia* subgenus *Chamaesyce* (Euphorbiaceae). *J. Exp. Bot.* 62:3183–95

125. Schulze E-D, Hall AE. 1982. Stomatal responses, water loss and CO_2 assimilation rates of plants in contrasting environments. In *Physiological Plant Ecology II: Water Relations and Carbon Assimilation*, Encycl. Plant Physiol. Vol. 12B, ed. O.L. Lange, P.S. Nobel, C.B. Osmond, H. Zieger, pp. 181–230. Berlin: Springer-Verlag

126. Scoffoni C, Rawls M, McKown A, Cochard H, Sack L. 2011. Decline of leaf hydraulic conductance with dehydration: relationship to leaf size and venation architecture. *Plant Physiol.* 156:832–43

127. Segalen L, Renard M, Lee-Thorp JA, Emmanuel L, Le Callonnec L, et al. 2006. Neogene climate change and emergence of C_4 grasses in the Namib, southwestern Africa, as reflected in ratite ^{13}C and ^{18}O. *Earth Planet. Sci. Lett.* 244:725–34

106. Provides in-depth reviews of the molecular evolution of major C_4-cycle enzymes and the many variations of C_4 anatomy.

121. Provides a comprehensive overview of C_4 biochemistry, anatomy, physiology, ecology, and evolution.

128. Smith BN, Robbins MJ. 1975. Evolution of C_4 photosynthesis: an assessment based on $^{13}C/^{12}C$ ratios and Kranz anatomy. *Proc. 3rd Int. Congr. Photosynth. Res., Rehovot, Israel, 1974*, ed. M Avron, pp. 1579–87. Amsterdam: Elsevier

129. Still CJ, Berry JA, Collatz GJ, DeFries RS. 2003. Global distribution of C_3 and C_4 vegetation: carbon cycle implications. *Glob. Biogeochem. Cycles* 17:1006–30

130. Stromberg CAE. 2004. Using phytolith assemblages to reconstruct the origin and spread of grass-dominated habitats in the great plains of North America during the late Eocene to early Miocene. *Palaeogeogr. Palaeoclimatol. Palaeoecol.* 207:239–75

131. Stromberg CAE. 2011. Evolution of grasses and grassland ecosystems. *Annu. Rev. Earth Planet. Sci.* 39:517–44

132. Sudderth EA, Espinosa-Garcia FJ, Holbrook NM. 2009. Geographic distributions and physiological characteristics of co-existing *Flaveria* species in south-central Mexico. *Flora* 204:89–98

133. Tipple BJ, Pagani M. 2007. The early origins of terrestrial C_4 photosynthesis. *Annu. Rev. Earth Planet. Sci.* 35:435–61

134. Tripati AK, Roberts CD, Eagle RA. 2009. Coupling of CO_2 and ice sheet stability over major climate transitions of the last 20 million years. *Science* 326:1394–97

135. Ueno O, Yoshimura Y, Sentoku N. 2005. Variation in the activity of some enzymes of photorespiratory metabolism in C_4 grasses. *Ann. Bot.* 96:863–69

136. Uhl D, Mosbrugger V. 1999. Leaf venation density as a climate and environmental proxy: a critical review and new data. *Palaeogeogr. Palaeoclimatol. Palaeoecol.* 149:15–26

137. Urban MA, Nelson DM, Jimenez-Moreno G, Chateauneuf JJ, Pearson A, Hu FS. 2010. Isotopic evidence of C_4 grasses in southwestern Europe during the Early Oligocene–Middle Miocene. *Geology* 38:1091–94

138. Vicentini A, Barber JC, Aliscioni SS, Giussani LM, Kellogg EA. 2008. The age of the grasses and clusters of origins of C_4 photosynthesis. *Glob. Change Biol.* 14:2963–77

139. Vogan PJ, Frohlich MW, Sage RF. 2007. The functional significance of C_3-C_4 intermediate traits in *Heliotropium* L. (Boraginaceae): gas exchange perspectives. *Plant Cell Environ.* 30:1337–45

140. Vogan PJ, Sage RF. 2011. Water-use efficiency and nitrogen-use efficiency of C_3-C_4 intermediate species of *Flaveria* Juss. (Asteraceae). *Plant Cell Environ.* 34:1415–30

141. Vogan PJ, Sage RF. 2012. Effects of low atmospheric CO_2 and elevated temperature during growth on the gas exchange responses of C_3, C_3-C_4 intermediate, and C_4 species from three evolutionary lineages of C_4 photosynthesis. *Oecologia.* In press; doi:10.1007/s00442-011-2201-z

142. Von Caemmerer S. 1989. A model of photosynthetic CO_2 assimilation and carbon-isotope discrimination in leaves of certain C_3-C_4 intermediates. *Planta* 178:463–74

143. Von Caemmerer S. 1992. Carbon isotope discrimination in C_3-C_4 intermediates. *Plant Cell Environ.* 15:1063–72

144. Von Caemmerer S. 2000. *Biochemical Models of Leaf Photosynthesis*. Collingwood, Australia: CSIRO

145. Voznesenskaya EV, Artyusheva EG, Franceschi VR, Pyankov VI, Kiirats O, et al. 2001. *Salsola arbusculiformis*, a C_3-C_4 intermediate in Salsoleae (Chenopodiaceae). *Ann. Bot.* 88:337–48

146. Voznesenskaya EV, Koteyeva NK, Chuong SDX, Ivanova AN, Barroca J, et al. 2007. Physiological, anatomical and biochemical characterisation of photosynthetic types in genus *Cleome* (Cleomaceae). *Funct. Plant Biol.* 34:247–67

147. Voznesenskaya EV, Koteyeva NK, Edwards GE, Ocampo G. 2010. Revealing diversity in structural and biochemical forms of C_4 photosynthesis and a C_3-C_4 intermediate in genus *Portulaca* L. (Portulacaceae). *J. Exp. Bot.* 61:3647–62

148. Wang XY, Gowik U, Tang HB, Bowers JE, Westhoff P, Paterson AH. 2009. Comparative genomic analysis of C_4 photosynthetic pathway evolution in grasses. *Genome Biol.* 10:R68

149. Willis KJ, McElwain JC. 2002. *The Evolution of Plants*. Oxford, UK: Oxford Univ. Press

150. Winter K, Smith JAC, eds. 1996. *Crassulacean Acid Metabolism: Biochemistry, Ecophysiology and Evolution*. Ecol. Stud. 114. Berlin: Springer

151. Wright VP, Vanstone SD. 1991. Assessing the carbon-dioxide content of ancient atmospheres using palaeocalcretes: theoretical and empirical constraints. *J. Geol. Soc.* 148:945–47

129. A detailed synopsis of C_4 productivity patterns across the globe.

131. A comprehensive paleoecology review of the origins of C_4 grasslands and savannas.

152. Zachos JC, Dickens GR, Zeebe RE. 2008. An early Cenozoic perspective on greenhouse warming and carbon-cycle dynamics. *Nature* 451:279–83
153. Zachos JC, Pagani M, Sloan L, Thomas E, Billups K. 2001. Trends, rhythms and aberrations in global climate 65 Ma to present. *Science* 292:686–993
154. Zuloaga FO, Morrone O, Vega AS, Giussani LM. 1998. Revision and cladistic analysis of *Steinchisma* (Poaceae: Panicoideae: Paniceae). *Ann. Mo. Bot. Garden* 85:631–56

Annual Review of
Plant Biology
Volume 63, 2012

Contents